Carbohydrate Polymers 320 (2023) 121194

Contents lists available at ScienceDirect

Carbohydrate Polymers

journal homepage: www.elsevier.com/locate/carbpol

Tip loaded cyclodextrin-carvedilol complexes microarray patches

Qonita Kurnia Anjani [a,b], Akmal Hidayat Bin Sabri [a], Khuriah Abdul Hamid [c], Natalia Moreno-Castellanos [d], Huanhuan Li [a], Ryan F. Donnelly [a,*]

[a] School of Pharmacy, Queen's University Belfast, Medical Biology Centre, 97 Lisburn Road, Belfast BT9 7BL, UK
[b] Fakultas Farmasi, Universitas Megarezky, Jl. Antang Raya No. 43, Makassar 90234, Indonesia
[c] Department of Pharmaceutics, Faculty of Pharmacy, Universiti Teknologi MARA Cawangan Selangor, 42300 Puncak Alam, Malaysia
[d] Basic Science Department, Faculty of Health, Universidad Industrial de Santander, Bucaramanga 680001, Colombia

ARTICLE INFO

Keywords:
Cyclodextrin
Carvedilol
Ternary inclusion complexes
Microarray patches
Heart failure

ABSTRACT

Carvedilol, a β-blocker prescribed for chronic heart failure, suffers from poor bioavailability and rapid first pass metabolism when administered orally. Herein, we present the development of tip microarray patches (MAPs) composed of ternary cyclodextrin (CD) complexes of carvedilol for transdermal delivery. The ternary complex with hydroxypropyl γ-cyclodextrin (HPγCD) and poly(vinyl pyrrolidone) (PVP) reduced the crystallinity of carvedilol, as evidenced by DSC, XRD, NMR, and SEM analysis. MAPs were fabricated using a two-step process with the ternary complex as the needle layer. The resulting MAPs were capable of breaching *ex vivo* neonatal porcine skin to a depth ≈600 μm with minimal impact to needle height. Upon insertion, the needle dissolved within 2 h, leading to the transdermal delivery of carvedilol. The MAPs displayed minimal toxicity and acceptable biocompatibility in cell assays. In rats, MAPs achieved significantly higher AUC levels of carvedilol than oral administration, with a delayed T_{max} and sustained plasma levels over several days. These findings suggest that the carvedilol-loaded dissolving MAPs have the potential to revolutionise the treatment of chronic heart failure.

1. Introduction

Heart failure is a progressive multi-faceted cardiovascular condition characterised by reduced cardiac output of the heart (Schwinger, 2021). Generally, the reduction in the efficiency of the heart muscle to pump or fill with blood may arise from a multitude of factors, ranging from myocardial infarction, hypertension or even rarely, cardiac amyloidosis (Grogan & Dispenzieri, 2015). The progression of this condition coupled with the prevalence of this disease can result in significant morbidity and mortality at a global scale. A comprehensive Global Burden of Diseases, Injuries, and Risk Factors Study in 2017 estimated that over 64 million individuals worldwide suffers from heart failure which amounts to a staggering 9.91 million years lived with disability (YLD) (Savarese & Lund, 2017). The situation is further exacerbated by ever rising number of geriatric populations which have a higher predisposition in developing chronic heart failure (Dodson & Chaudhry, 2012).

According to the National Institute for Health and Care Excellence (NICE), the first line pharmacotherapy for heart failure involves a combination of angiotensin-converting enzyme (ACE) inhibitor and a β-blocker. Some of the common ACE inhibitor used in the management of heart failure include perindopril, ramipril, captopril, enalapril maleate, lisinopril, quinapril and fosinopril sodium. On the other hand, the range of β-blockers licensed for heart failure include nebivolol, carvedilol and bisoprolol fumerate (National Institute for Health and Care Excellence, 2018). There are currently three generations of β-blocker used in the management of heart failure with the later displaying the highest selectivity for β1-receptors while also exhibiting some levels of vasodilation by acting upon the α1-adrenoreceptors and β3-adrenergic receptors which is beneficial in the management of chronic cardiovascular conditions (Do Vale et al., 2019).

One of the third generation of β-blockers is carvedilol. Relative to other β-blockers, carvedilol exhibits a much greater adrenergic inhibition while conferring significant vasodilating and antioxidative properties (Eichhorn & Bristow, 2001; Investigators, 2001; Poole-Wilson et al., 2003). Despite these pharmacological advantages, the oral bioavailability of carvedilol is limited (25–35 %) and exhibits significant interpatient variability (Sharma et al., 2019a). Such variability arises from its narrow absorption window within the upper gastrointestinal

* Corresponding author at: School of Pharmacy, Queen's University Belfast, Medical Biology Centre, 97 Lisburn Road, Belfast BT9 7BL, Northern Ireland, UK.
E-mail address: r.donnelly@qub.ac.uk (R.F. Donnelly).

https://doi.org/10.1016/j.carbpol.2023.121194
Received 3 May 2023; Received in revised form 27 June 2023; Accepted 9 July 2023
Available online 11 July 2023

tract, slow dissolution profile and significant level of hepatic first pass metabolism (Sharma et al., 2019a). Given this limitation with the oral delivery of carvedilol, formulators have begun exploring alternative routes of administering this third generation β-blocker (Tanwar et al., 2007; Zaid Alkilani et al., 2018), which showed that delivering the β-blocker *via* the transdermal route may offer a potential solution to improve the bioavailability of the drug. One transdermal drug delivery strategy that has yet to be explored for the delivery of carvedilol is *via* the use microneedle patches or microarray patches (MAPs). These are micron size projections on a flat baseplate which can disrupt the *stratum corneum* (SC) upon skin application. The disruption of the SC, the protective outermost layer of the skin, by MAPs also generates micron size channels which can be utilised for the delivery of small drug molecules and even macromolecules into and across the skin (Ripolin et al., 2017).

One of the most common types of MAPs used in drug delivery are dissolving MAPs. These consist of microneedles that are fabricated from water soluble matrices such poly(vinyl pyrrolidone) (PVP), poly(vinyl alcohol) (PVA) or even saccharides (Vora et al., 2021). Upon skin application, the needle layers will undergo dissolution leading to the deposition drug loaded needle tips within the skin strata (Anjani et al., 2022a). These needles will then undergo dissolution due to the presence of surrounding dermal interstitial fluid which will lead to the release of the payload into the surrounding dermal tissues (Anjani et al., 2022b).

In this present study, we utilised carvedilol ternary complexes to fabricate needle tips, aiming to enhance the transdermal delivery and bioavailability of carvedilol for the management of heart failure. The solubility and stability of carvedilol were improved through carvedilol-cyclodextrin (CD) complexation and the development of a ternary complex with suitable polymers (PVP or PVA). By employing dissolving MAPs as a transdermal drug delivery strategy, we achieved efficient delivery of carvedilol through the skin, resulting in enhanced and sustained systemic delivery of the β-blocker. Although there have been a few existing researches that detailed the use of cyclodextrins in the fabrication of dissolving MAPs (He et al., 2023; Lin et al., 2019; Yao et al., 2017), these studies mainly employed cyclodextrin for the purpose of enhancing the solubility of poorly soluble drug as well as enhancing the overall mechanical properties of the MAP. In doing so, the researchers demonstrated that cyclodextrin could be used to produce strong MAPs which are capable of breaching tough skin conditions, such as scars. However, these previous studies failed to demonstrate how these cyclodextrin complexes, backed by strong spectroscopic evidence, interact with other polymeric excipients within the tips of the MAPs. Therefore, one of the main novelties in the current work, is our ability to demonstrate in detail how ternary complexes are formed in the tip MAPs. Furthermore, this current work also demonstrates for the first time that these ternary cyclodextrin complexes that are generated in the tip of the MAPs can serve as intradermal depot, upon skin application, for the sustained release of poorly soluble drug such carvedilol over several days. This novel approach offers a patient-friendly and painless method for improving the bioavailability of carvedilol, ultimately contributing to the effective management of heart failure.

2. Materials and methods

2.1. Materials

Carvedilol ($C_{24}H_{26}N_2O_4$) (MW 406.5 g/mol, purity >98 %) was purchased from Tokyo Chemical Industry (Oxford, UK). Cavasol™ W7 HP Pharma (hydroxypropyl-βCD) ($C_{63}H_{112}O_{42}$) (MW 1410 g/mol), Cavasol™ W8 HP Pharma (hydroxypropyl-γCD) ($C_{72}H_{128}O_{48}$) (MW 1540 g/mol), Plasdone™ K-29/32 or Poly(vinyl pyrrolidone) (PVP) $(C_6H_9NO)_n$ (MW 58,000 g/mol) and PVP K-90 (MW 1,300,000 g/mol) were kindly provided by Ashland (Kidderminster, UK). Poly(vinyl alcohol) (PVA) $(C_2H_4O)_n$, 80 % hydrolysed (MW 9000–10,000 g/mol) was purchased from Sigma-Aldrich (Dorset, UK). Other chemicals and materials were of analytical grade and were bought from Sigma-Aldrich (Dorset, UK) and Fisher Scientific (Leicestershire, UK). Full-thickness and dermatomed neonatal porcine skin were collected from stillborn piglets in <24 h *post-mortem*. The skin was stored at −20 °C prior to use.

2.2. Saturation solubility

Saturation solubility experiments were conducted to determine the solubility of carvedilol in various aqueous media. To do this, an excessive quantity of carvedilol was dispersed into Eppendorf tubes containing 2 mL of different aqueous media such as deionized water, phosphate buffer solution (PBS) with a pH of 7.4, or deionized water with HPGCD 1 % *w/v*. These samples were stored in a shaker incubator (Jeio Tech ISF-7100, Medline Scientific, Chalgrove Oxon, UK) at a stirring speed of 100 rpm and a temperature of 37 °C for 24 h. Before analysis, the samples were centrifuged at 15,300 rpm for 15 min and then filtered using 0.45 μm syringe filters (Agilent Technologies, Agilent UK Ltd., Stockport, UK). If needed, the samples were appropriately diluted and assessed using the verified HPLC method described in Section 2.14.

2.3. Phase solubility and constant calculation

The same technique as saturation solubility studies (Section 2.2) was used to conduct phase solubility studies, but CD solutions at varying concentrations were employed. A series of CD solutions were made at 10, 20, 30, 40, and 50 mM for HP-βCD and HP-γCD, respectively. The solubility of carvedilol was determined and presented in a graph where the concentration of CD and carvedilol were plotted on the x-axis and y-axis, respectively.

The binding constant (Ks) was calculated using Eq. (1) by means of linear regression of a phase solubility diagram to assess the strength of CD's interaction with carvedilol.

$$Ks = \frac{slope}{S_0 \bullet (1 - slope)} \tag{1}$$

The complexation efficiency was calculated using slope of the linear regression as shown in Eq. (2).

$$CE = \frac{slope}{1 - slope} \tag{2}$$

Based on CE calculation, the molar ratio of carvedilol:CD was calculated using Eq. (3).

$$CAR : CD\ molar\ ratio = 1 : \frac{(CE + 1)}{CE} \tag{3}$$

2.4. Optimisation of CD complexation

In this study, PVA 9–10 kDa and PVP 58 kDa were selected to create carvedilol-CD ternary complexes. A design of experiments (DoE) approach, specifically the central composite design (CCD), was utilised to evaluate the effect of HPγCD and PVA/PVP on the solubility of carvedilol. HPγCD and PVA/PVP concentrations were the factors considered, and carvedilol solubility was the response of the design. The assigned concentrations of HPγCD and PVA/PVP were utilised to create the ternary complexes. Carvedilol was set at a fixed concentration of 2 % *w/v* for all the designed ternary complexes, and its solubility was measured in triplicate. The impact of HPγCD and PVA/PVP concentrations on carvedilol solubility in ternary complexes was assessed using a fitted model (Loftsson et al., 1996).

2.5. Preparation of ternary complexes of carvedilol/HPγCD/PVP and carvedilol/HPγCD/PVA

The method of preparing carvedilol complexes involved a freeze-drying technique that was slightly modified from a previously

reported method (Anjani et al., 2021a). First, HPγCD powder was dissolved in a PVP solution, with PVP concentrations ranging from 0.2 % to 2 % *w/v*. The mixture was homogenised using a SpeedMixer™ for 5 min at 3500 rpm. Carvedilol powder was then added to the solution and mixed again at 3500 rpm for 5 min. The resulting solution was frozen at −80 °C for 3 h and then transferred to a freeze drier where it was kept for 24 h inside a vacuum chamber with a pressure of 50 mTorr. The process involved primary drying for 13 h at a shelf temperature starting from −40 °C, followed by secondary drying for 11 h at 25 °C.

2.6. Characterisation of inclusion complexes

The physicochemical properties of the drug/CD/polymer complex were investigated by subjecting the ternary complex powder to a series of characterisation experiments. The chemical interactions between carvedilol, HPγCD and PVP were investigated using a Fourier transform infrared (FTIR) spectrometer (Accutrac FT/IR-4100™ Series, Perkin Elmer, USA). The crystallinity of pure carvedilol, pure HPγCD, pure PVP, physical mixture (PM) and ternary complex powder were determined using a differential scanning calorimeter DSC Q20 (TA Instruments, Elstree, Hertfordshire, UK) and an X-ray diffractometer (Rigaku Corporation, Kent, England). The structure and morphology of the pure drug and excipient as well as the complex powder were visualised *via* scanning electron microscopy (SEM) analysis with a TM3030 microscope (Hitachi, Krefeld, Germany). Prior to analysis, the samples were left to dry for 24 h under ambient conditions. In addition, the complexation was also evaluated *via* proton nuclear magnetic resonance (NMR) ^{1}H NMR, in which samples were dissolved in Dimethyl sulfoxide-d6. The NMR spectra were recorded using Bruker Ultrashield 400 spectrometer (Bruker, Leipzig, Germany) operated at 400 MHz. The NMR spectra were processed with MestReNova 6.0.2© (Mestrelab Research, Santiago de Compostela, Spain). All chemical shifts are reported in ppm (δ) relative to tetramethylsilane or referenced to the chemical shifts of residual solvent resonances.

2.7. Fabrication of dissolving MAPs

The authors employed a two-step casting method, previously described, to create MAPs containing a carvedilol ternary complex (Kurnia et al., 2022). In this process, a mixture of the complexed powder and water (in a 1:2 ratio) was cast into a silicone mould with 16 × 16 pyramidal needles, resulting in a 850 μm high layer with a width of 300 μm at the base, 300 μm interspacing, and a patch area of 0.36 cm^2. The details of this layer's composition can be found in Table 1. After 5 min of exposure to a positive pressure of 4 bar in a closed chamber, any excess formulation was removed, and the first casted layers were left to air dry, forming the needle layer of the patch. Next, silicone rings (with an external diameter of 23 mm, internal diameter of 18 mm, and thickness of 3 mm) were added to the moulds, secured by 40 % *w*/w PVA (9–10 kDa). Then, a baseplate solution composed of 30 % w/w PVP (90 kDa) and 1.5 % w/w glycerol was poured onto the needle layer. After drying and demoulding, the patch was left in a 37 °C oven for an additional 12 h to eliminate any remaining moisture from the MAPs.

Table 1
Formulations for first layer of dissolving MAP preparation.

MAP formulation code	Concentration of PVP solution added to the complex powder (% *w/v*)
F1	–
F2	0.2
F3	0.4
F4	1
F5	2

2.8. Assessment of mechanical and insertion properties of dissolving MAPs

The shape and structure of the manufactured MAPs were examined using a stereo microscope (Leica EZ4 D, Leica Microsystems, Milton Keynes, UK) and scanning electron microscopy (SEM), TM3030 microscope (Hitachi, Krefeld, Germany). To determine the patch's ability to withstand force during skin application, the MAPs were compressed with a force of 32 N using a TA-TX2 Texture Analyser (TA) (Stable Microsystems, Haslemere, UK) according to previous methods (Sabri et al., 2021). After compression, changes in MAP height were measured using Eq. (4).

$$\textit{Change in needle height}\ (\%) = \frac{\Delta \textit{needle height}}{\textit{original needle height}} \text{x } 100 = \frac{H_a - H_b}{H_a} \times 100\% \quad (4)$$

where H_a denotes needle height before compression and H_b denotes needle height post compression.

The capability of the MAPs to be inserted into the skin was assessed by inserting them into eight layers of Parafilm® M, which was chosen as a skin simulation material for this study (Larrañeta et al., 2014). In addition, an insertion test was conducted using neonatal porcine skin of full thickness *ex vivo*. The needle insertion was observed *in situ* using an EX-101 optical coherence tomography (OCT) microscope (Michelson Diagnostics Ltd., Kent, UK). The OCT images were collected and analysed using ImageJ® (National Institutes of Health, Bethesda MD, USA) to determine the depth of needle penetration.

2.9. Calculation of drug content localised in the needles

The dissolving MAPs were dissolved in deionized water (4 mL) and placed in an ultrasonic bath for 30 min. Methanol (4 mL) was added to the mixture and sonicated for another 30 min. 2 mL of the mixture were taken into an Eppendorf tube and centrifuged at 14,500 rpm for 15 min. The supernatants were collected and then diluted with methanol before undergoing HPLC analysis.

2.10. MAP dissolution study in full thickness skin

Full-thickness neonatal porcine skin was soaked in PBS with pH 7.4 for 30 min prior to experiment. The surface of the skin (the *stratum corneum* side) was dried using a paper towel. The MAPs, (F1–F5), were inserted into the skin using thumb pressure for 30 s, and cylindrical weights made of stainless steel (weighing 15.0 g) were placed on top of the patch to prevent it from dislodging from the skin after insertion. The skin with the MAPs inserted was placed in an oven at 37 °C, which was thermostatically controlled. At 0.5, 1.0, and 2.0 h, the MAPs were removed from the skin with care, and the length of the needles on the MAPs were observed and recorded using a digital microscope.

2.11. In vitro permeation study

The permeation of carvedilol into and across the skin was evaluated using a Franz diffusion cells (Permergear, Hellertown PA, USA) set up. PBS (pH 7.4) that was degassed and pre-warmed to 37 ± 1 °C was added to the receiver chamber. Using a thermostatically controlled water bath, the temperature of the receiver chamber was maintained at 37 ± 1 °C throughout the duration of the experiment. The donor chamber (28 mm-diameter) was assembled by attaching excised full thickness neonatal porcine skin to the compartment using cyanoacrylate glue. Carvedilol/CD/PVP loaded dissolving MAPs as applied to the skin by pressing the patch using thumb pressure for 0.5 min, followed by the addition of a 5.0 g cylindrical stainless-steel weight as previously reported (Anjani et al., 2022c). At pre-determine intervals over the course of 24 h, the

receiver chambers were sampled, and equal volume of fresh PBS was replaced into the receiver compartment. After 24 h, the release media and skin samples were carefully collected, processed, and analysed *via* HPLC analysis, as previously reported (Anjani et al., 2022d).

2.12. Biocompatibility study

A series of biocompatibility assays were conducted to evaluate the biocompatibility of dissolving MAPs loaded with carvedilol/CD/PVP and CD/PVP alone with fibroblast cells (ATCC CL-173). The cells were cultured in DMEM growth media supplemented with 10 % fetal bovine serum (*v*/v), 1 % sodium pyruvate (v/v), and 1 % antibiotic–antimycotic solution (v/v) containing penicillin, streptomycin, and amphotericin B. The fibroblast cells were plated onto a 24-well plate and incubated with the formulation for 72 h at 37 °C with 5 % CO_2 under a 60 % humidified atmosphere. In addition, cell compatibility of carvedilol/CD/PVP loaded dissolving MAPs was evaluated by methyl thiazolidazole tetrazolium (MTT) assay as was described before (Anjani et al., 2022a; Anjani et al., 2022b). In addition, cell viability was evaluated using LIVE/DEAD™ staining as was described previously (Utomo et al., 2022). Following the staining protocol, fluorescence images were taken using an Olympus Fluoview Confocal Microscope (Olympus America, USA). Further to this, the proliferation profiles of the cells following exposure to the formulation was evaluated using the PicoGreen assay after 72 h treatment to the formulation, as previously described (Anjani et al., 2022b).

2.13. Pharmacokinetic study

Six male Sprague Dawley rats weighing 300–350 g were obtained from the Laboratory Animal Facility and Management (LAFAM), Universiti Teknologi MARA (UiTM) Puncak Alam, Selangor, Malaysia. The animal experiments were conducted following the guidelines of the Committee on Animal Research & Ethics (CARE) of the Faculty of Pharmacy, UiTM. The rats were sedated using an intraperitoneal injection (IP) of Zoletil®50 (0.1 mL/100 g rat weight) and their back fur was shaved with electric clippers. After complete fur removal, four dissolving MAPs were applied to the back of each rat and secured in place with Microfoam™ surgical tape (3M, Bracknell, UK), and then Kinesiology™ tape (Proworks, Stockton, UK). The MAP was left in place for 24 h before being removed. For the oral treatment group, the rats were fasted overnight and then administered 1 mg/kg of carvedilol *via* oral gavage. Blood samples were taken from the tail vein at predetermined time intervals using a heparinised syringe with needle and the plasma was frozen at −80 °C until further analysis. To determine the effect of the formulation on the lumen diameter of the aorta, the hearts of the rats were collected post-mortem and fixated using 10 % aqueous mixture of neutral buffered formalin. The aorta of the rats' hearts were sectioned, stained with haematoxylin and eosin (H&E), and mounted with a coverslip using optical grade glue.

2.14. HPLC method

2.14.1. In vitro study

A previously reported method was used to perform the analysis of carvedilol samples using a UV detector in reversed phase HPLC on an Agilent Technologies 1220 Infinity Compact LC series system (Agilent Technologies UK Ltd., Stockport, UK) (Anjani et al., 2022d). Chromatographic separation was achieved using an XSelect CSH C18 column (3.0 mm internal diameter, 150 mm length, 3.5 μm particle size and a pore size of 130 Å) from Waters (Dublin, Ireland) with a VanGuard® cartridge (3.9 mm internal diameter, 5 mm length) from Waters (Dublin, Ireland) preceding the main column. The mobile phase consisted of 0.1 % *v*/v trifluoroacetic acid in water and acetonitrile (65:35) with a flow rate of 0.6 mL/min. The HPLC samples were analysed at 30 °C with an injection volume of 10 μL and detection of the analyte was done at 210 nm. The overall sample analysis time was 8 min.

2.14.2. In vivo study

A rapid and precise method for measuring carvedilol in rat plasma was established using UHPLC-MS/MS technology. The UHPLC-MS/MS system used was composed of an Agilent 1200 infinity UHPLC system with an Agilent 6460 triple-quadrupole mass spectrometer, controlled by Agilent Mass Hunter Workstation Data Acquisition system. Chromatographic separation was performed at 40 °C using an Zorbax SB-C18 Rapid Resolution HT (2.1 m × 50 mm, 1.8 μm) with (A) 0.1 % formic acid in water and (B) methanol. The sample injection volume was 2 μL and the flow rate was set at 0.250 mL/min. A calibration curve was prepared with 200 μL of blank rat plasma spiked with both standards at different concentrations. For plasma extraction, 100 μL of the sample was mixed with 10 μL of internal standard (ketoconazole) and 1 mL of ethyl acetate to precipitate the protein. After centrifugation, 950 μL of the supernatant was transferred to a new microcentrifuge tube and dried using a benchtop centrifugal evaporator. The dried sample was then reconstituted with 50 μL of 50 % methanol in ddH_2O with 0.1 % added, followed by vortex mixing and centrifugation. The resulting supernatant was injected into the LC/MS-QQQ system for analysis.

2.15. Statistical analysis

The statistical analysis of the data was conducted using GraphPad Prism® version 8.0 (GraphPad Software, San Diego, California, USA). The data is presented as means ± standard deviation (SD), unless specified otherwise. One-way analysis of variance (ANOVA) was used to compare multiple groups in saturation solubility studies, evaluation of drug content of powder complexes and loaded in MAPs, needle height reduction, parafilm insertion studies, skin and parafilm insertion depth, drug deposited and permeated across the porcine skin, and cell studies. A p-value of <0.05 was considered statistically significant for all analyses.

3. Results and discussion

3.1. Saturation solubility study and development of ternary inclusion complexation of carvedilol with cyclodextrin

Prior to any formulation development and optimisation, a saturation solubility study of carvedilol in different aqueous media was investigated. It can be seen from Fig. 1(A) that carvedilol possesses an aqueous solubility which is <5 μg/mL in deionized water and PBS (pH 7.4). In addition, the presence of CD, HPβCD in deionized water did not improve the aqueous solubility of the drug, which suggests that the drug does not readily form a complex with HPβCD. This observation agrees with the reported physiochemical properties of carvedilol that described the drug as lipophilic due to the presence of the carbazole and phenyl groups that culminate in its low aqueous solubility (Loftsson et al., 2008a). However, it was apparent that the addition of the excipient Tween® 80 did improve the solubility of the β-blocker significantly ($p < 0.05$). This may be attributed to the role of Tween® 80 as a surfactant that lowers the surface tension at the solid−liquid interface between carvedilol and PBS (pH 7.4), thus augmenting the spread and penetration of liquid into solid drug particles (Paria et al., 2012). Nevertheless, such enhancement in solubility, due to the addition of surfactant, was only ≈10 folds. This observation echoes with our previous work that showed that the addition of surfactant in the manufacture of dissolving MAPs was not a viable strategy to promote enhancement in drug loading, despite conferring improvement in mechanical properties of MAP, as well as the drug release profile of the drug across the skin (Anjani et al., 2022e).

Given this limitation, we then proceeded to explore the utility of cyclodextrin as a solubility enhancement strategy for carvedilol prior to the development of dissolving MAP. In our previous work it has been shown that that hydroxypropyl-β cyclodextrin (HPβCD) and

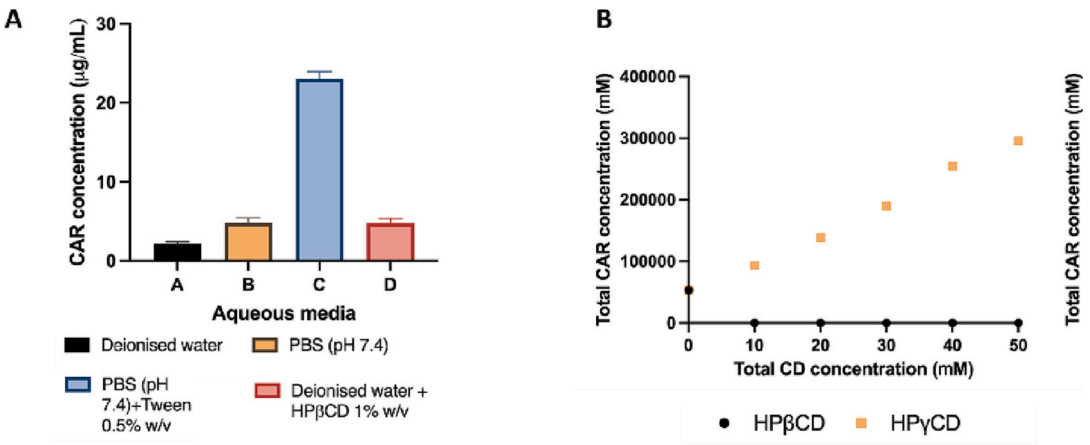

C

CAR form	CD type	Type of diagram	R^2	Intercept	Slope	Ks (mM^{-1})	CE	CAR:CD Molar ratio
Base	HP-βCD	-	-	-	-	-	-	-
	HP-γCD	AL	0.994	46.143	4.990	0.023	1.251	1: 2

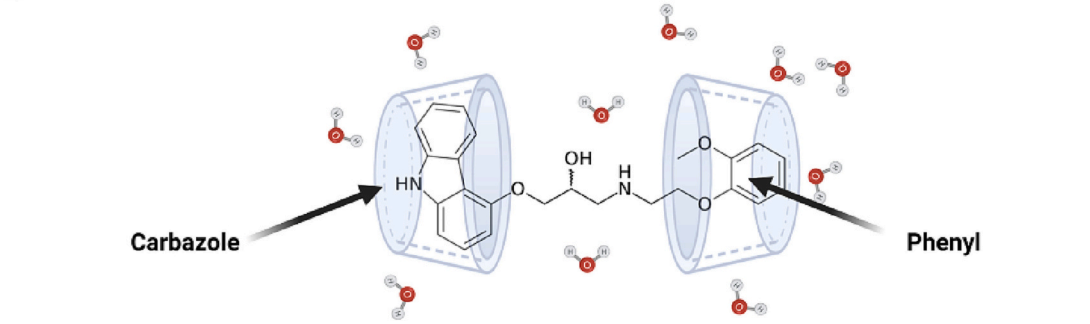

Fig. 1. (A) Saturation solubility of carvedilol in different aqueous media (Means + SD, $n = 4$). (B) Phase solubility diagrams of carvedilol (CAR) with HP-βCD, and HP-γCD. (C) Phase solubility data: slope and intercept, binding constant (Ks), complexation efficiency (CE), and carvedilol:CD molar ratio. (D) Proposed complexation between HP-γCD and carvedilol.

hydroxypropyl-γCD(HPγCD) were among the most effective macrocyclic oligosaccharides capable of enhancing the solubility of the poorly water-soluble drug rifampicin (Anjani et al., 2022f). In the current work, we evaluated if HPβCD and HPγCD would be capable of forming complex with carvedilol, thus leading to enhancement in aqueous solubility. This was first done by evaluating the phase solubility profiles attained from the complexation of carvedilol with either HPβCD or HPγCD. The results presented in Fig. 1(B) indicate that the solubility of carvedilol increased in a linear fashion with the concentration of HPγCD. In contrast, no enhancement in solubility of carvedilol was observed with increasing concentration of HPβCD. Based on the phase solubility classification introduced by Higuchi and Connors (Higuchi & Connor, 1965), the solubility curve following CD complexation can be divided into two main groups, namely type A and type B. Some of the cardinal features of type A solubility curves include an increase in in apparent solubility of the substrate, in this instance the drug, with an increase in ligand, in this instance CD, concentration (Saokham et al., 2018). On the other hand, the phase solubility diagram is classified as type B. if the addition of CD results in a plateau which then exhibit a decrease in solubility with an increase in CD concentration (Saokham et al., 2018). It should be noted that the molecular weight of carvedilol used in this study is 406.474 g/mol, while the inner cavity of HPγCD and HPβCD are 0.80 nm and 0.62 nm respectively (Wüpper et al., 2021). We have previously shown that both HPγCD and HPβCD are capable of forming inclusion complex with cabotegravir sodium which has a molecular weight of 428.347 g/mol (Volpe-Zanutto et al., 2022). As the molecular weight of carvedilol is smaller to that of cabotegravir sodium, it could be postulated that the annulus of both cyclodextrin is capable of accommodating carvedilol.

Based on the results in Fig. 1(B, C), the complexation between carvedilol with HPβCD results in the formation of type B_I phase solubility, indicating that the complex is insoluble (Higuchi & Connor, 1965). In contrast, carvedilol complexation with HPγCD resulted in a type A_L phase solubility, where L denotes linear with no deviation (Saokham et al., 2018). By calculating, the complexation efficacy (CE) *via* the slope of the phase solubility, we then proceed to estimate the ratio of carvedilol:HPγCD needed to form the complex. As shown in Fig. 1(C), it is estimated that two HPγCD would form a complex with one molecule of carvedilol (Anjani et al., 2021a). It has been reported that γCD possesses a much wider hydrophobic cavity, 8.5 Å relative to βCD, 7.0 Å, enabling large hydrophobic moieties to be accommodated into the CD annulus (Tsuchido et al., 2017). The formation of an insoluble complex can be attributed to the use of HPβCD, which has a cavity size that can only fit one smaller hydrophobic structure of carvedilol (Loftsson et al., 2008b; Loftsson & Brewster, 2010), likely the terminal phenyl group, but not the larger carbazole end group. As a result, the carbazole group was exposed, leading to the precipitation of the complex in aqueous conditions. In contrast, when HPγCDs were used, two CD molecules were able

to complex with one carvedilol molecule, which prevented the exposure of the carbazole group and the resulting precipitation of the complex (Loftsson & Brewster, 2010). This may occur when one molecule HPγCD chelates with the phenyl group on carvedilol while the other HPγCD is able to accommodate the hydrophobic carbazole group as shown in Fig. 1(D). This mitigates the exposure of any hydrophobic structure within an aqueous milieu thus enhancing the solubility of the β-blocker.

It was identified that HPγCD can form a water-soluble inclusion complex with carvedilol, resulting in an enhancement of the drug's water solubility. To further optimize the solubility of the inclusion complex, we proceeded to develop a multicomponent or ternary cyclodextrin complex by adding an auxiliary excipient. Loftsson et al. (1996) introduced the concept of adding small amounts of water-soluble polymers like PVP to binary mixtures of CD and poorly water-soluble drugs, thereby improving the overall solubility of the drug (Ravindran Maniam et al., 2022). The formation of these complexes is based on the affinity of CD for non-polar compounds and the dimensions of the guest compounds, as they follow the host-guest interaction. In the case of the CAR/HPγCD complex, it is a host-guest complex where only the host (HPγCD) is soluble in water, while the guest (CAR) has limited solubility in water. The ternary CAR/HPγCD/PVA or CAR/HPγCD/PVP complexes, formed by adding PVP to the complexes, can exhibit higher solubility compared to the binary complexes (CAR/HPγCD) due to the ready solubility of PVA or PVP in water. For this study, PVA and PVP were chosen as potential auxiliary components to develop a CD ternary complex. PVA and PVP were specifically selected as these polymers have been extensively used in the formulation of dissolving MAPs (Anjani et al., 2022e; Permana et al., 2020; Tekko et al., 2022) and have also been employed as a third component in multicomponent CD complexes (Bejaoui et al., 2019; Mora et al., 2015; Saokham et al., 2020).

A design of experiments (DoE) approach *via* central composite design (CCD) was used to methodically evaluate the effect of HPγCD and PVA/PVP on the solubility of carvedilol that entailed the use of 8 formulations that were suggested by the software as outlined in Tables S1 and S2. The solubility of carvedilol was recorded as the responses for all the ternary complexes developed, as presented in Fig. 2(A). From the Table in Fig. 2 (B) the predicted and observed carvedilol solubility for the different ternary complexes consisting of 2 % *w/v* of carvedilol, 2 % w/v of polymer and 2 % w/v HPγCD can be seen. It was observed that PVP conferred a significant higher enhancement ($p < 0.05$) in carvedilol solubility relative to PVA. This was true based on the predicted value from the software, as well as when the ternary complex was evaluated empirically. Furthermore, the bias of the predicted solubility enhancement was well below 15 %, suggesting the DoE model was accurate and successful (Anjani et al., 2021b; Kurnia et al., 2022). By comparing the results in Fig. 2(B) relative to observed solubility of carvedilol in Fig. 1 (A), the formation of a ternary complex with PVA resulted in ≈100-fold increase in solubility, while the formation of a ternary complex with PVP resulted in ≈200-fold enhancement in carvedilol solubility. This observation echoes with the early finding by Vieira et al. (2015), who observed that the addition of a water-soluble polymer, such as PVP, augmented CD complexation with a poorly soluble drug, leading to an improvement in the overall drug solubility (Vieira et al., 2015). This enhancement in solubility may be attributed to how the drug/CD complex interacts with the auxiliary excipient. For instance, Bejaoui et al. (2019) have shown via spectroscopic analysis the enhancement in intermolecular hydrogen-bonding and electrostatic interactions within a PVP/β-CD/ibuprofen ternary complex. This intermolecular interaction arises *via* the coating of PVP around the β-CD/ibuprofen complexes that culminated in the formation of a more water soluble and amorphous solid state which exhibit greater ibuprofen solubility (Bejaoui et al., 2019). Based on solubility enhancement data in Fig. 2(B), PVP was investigated further as an auxiliary excipient in the development of a ternary inclusion complex prior to MAP fabrication.

3.2. Characterisation of ternary inclusion complexes

A series of characterisation experiments on carvedilol/HPγCD were conducted with increasing PVP concentration (0–2 %) in order to investigate the impact of increasing polymer concentration on the

A

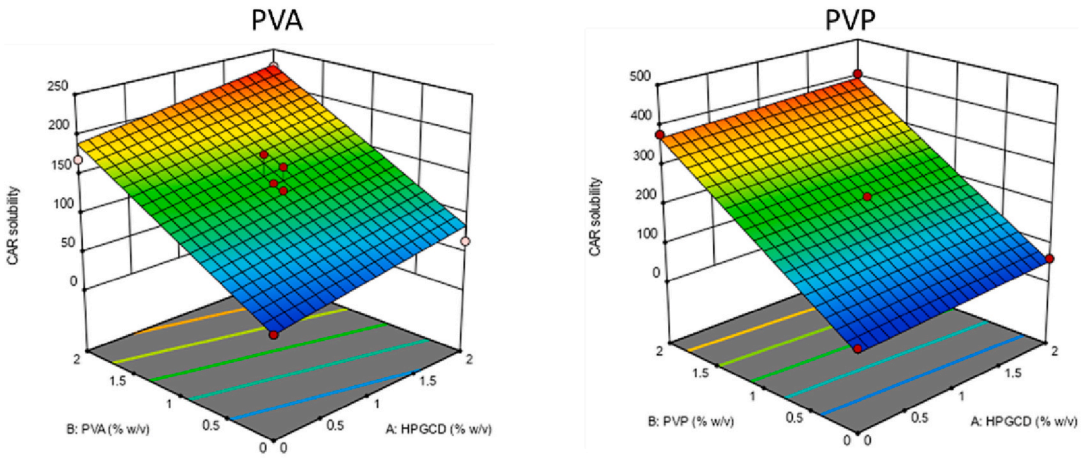

B

Factors			Response for CAR solubility		
HPGCD concentration (% w/v)	PVA concentration (% w/v)	PVP concentration (% w/v)	Predicted (μg/mL)	Observed (mean ± SD, n = 6) (μg/mL)	Bias (%)
2	2	-	228.781	209.33 ± 20.44	-7.94
2	-	2	394.983	385.02 ± 10.64	-2.52

Fig. 2. (A) Response surface plots detailing the effect HPγCD and polymer on the solubility of carvedilol (CAR) (B) Predicted and observed responses of the optimised CAR-HPγCD-polymer ternary complex.

properties of the ternary inclusion complex. The ternary complexes of carvedilol were prepared *via* lyophilization, as illustrated in Fig. 3(A). It can be seen that increasing the concentration of PVP to from a ternary complex with carvedilol/HPγCD did not impact the overall drug content per 1 mg of formulation ($p > 0.05$), as shown in Fig. 3(B). Next, the physiochemical properties of the ternary complex were investigated further *via* DSC analysis. The DSC thermograms Fig. 3(C) of pure carvedilol exhibit a clear endothermic peak at 120 °C. This correspond to the melting point of carvedilol when the drug is present in a crystalline state, as previously reported by Skotnicki et al. (2022). On the other hand, the thermal profile of HPγCD displayed a boarder endothermal peak at 120 °C, which corresponds to the dehydration of the excipient during the DSC heating cycle, as previously reported (Kim et al., 2010). In addition, the curves of the physical mixtures of the excipients and drugs, along with the complexes of carvedilol with HPγCD and PVP, are also displayed in Fig. 3(C). It was apparent that the addition of HPγCD and PVP to carvedilol retained the endothermic peak of the drug, which suggests no interaction between the excipients and the API. However, we observed a shift in temperature from 120 °C to 116 °C when complexation took place between carvedilol with HPγCD and PVP. Such a shift in endotherm for carvedilol has been attributed to a reduction in the crystallinity of the drugs along with a partial dispersion of the API at a molecular level within the lyophilised powder (Ribeiro et al., 2003). Besides the shift of the endotherm towards a lower temperature, we also observed that the intensity of the endotherm was also reduced when carvedilol was mixed and lyophilised with HPγCD and PVP. Such reduction in the intensity of the endotherm of API has been shown to be a cardinal sign that complexation has taken place between the drug and the excipients (Hirlekar & Kadam, 2009a).

In order to further investigate the solid-state characteristics of the formed ternary complex, XRD analysis was conducted on the pure drug, raw excipients, and the lyophilised complexation powders. The XRD diffraction pattern of the raw drug indicated that the carvedilol polymorph used in this study exists in form II, which is the anhydrous polymorph of carvedilol consisting only of the free base with a solubility profile previously reported (Prado et al., 2014). The distinguished peaks for pure carvedilol were observed at 5.84°, 15.32°, 17.52°, 24.82°, and 26.66°. As for the XRD pattern of pure HPγCD exhibited a sharp peak at 21.59°, while no Which mdistinct diffraction peaks for pure PVP, which indicating the amorphous state of PVP. In the diffractogram of the PM of carvedilol with HPγCD and PVP, it appeared as a combination of the API and the excipients, showing similar sharp peaks (at 20.62 and 24.74°) and interplanar distance. However, slight changes in peak positions, intensities, and small differences in the d values were observed in the diffractograms of the physical mixtures. This suggests that some level of interaction may have occurred within the physical mixture of the drug and excipients prior to complexation, a phenomenon previously reported by other researchers (Hirlekar & Kadam, 2009a). Upon formation of the ternary complex between CAR/HPγCD and PVP, a significant reduction in the intensity of the diffraction peaks for carvedilol was observed, with a more pronounced reduction at higher PVP concentrations. This indicates a decrease in the crystallinity of the drug upon complexation. The reduction in carvedilol crystallinity with higher PVP concentration can be attributed to the ability of water-soluble polymers to interact with the hydroxyl (—OH) groups on the outer surface of cyclodextrin drugs, leading to the formation of co-complexes with higher stability. This enhanced stability mitigates the tendency of the complexes to aggregate, thereby reducing the likelihood of drug recrystallisation (Loftsson et al., 2005).

FTIR analysis was conducted to further investigate the interaction between carvedilol, HPγCD, and PVP in the formation of a ternary inclusion complex. Carvedilol exhibited characteristic bands attributed to the carbazole structure at 1253 cm^{-1}, 1502 cm^{-1}, and 2922 cm^{-1}, as shown in Fig. 3(E). These wavenumbers correspond to the vibrations of aromatic secondary C—N, C—C, and C—H stretching of the aromatic carbazole ring on the drug molecule (Hirlekar & Kadam, 2009b). Additionally, the sharp band at 3340 cm^{-1} is attributed to the stretching of N—H and O—H groups present in the middle of the molecule. HPγCD displayed bands at around 3400 cm^{-1}, representing the stretching of hydroxyl groups (—OH), and at 2930 cm^{-1}, representing C—H stretching. It also exhibited a band at 1650 cm^{-1}, attributed to H—O—H bending (Yildiz et al., 2018). The FTIR spectra for PVP, as shown in Fig. 3(E), displayed peaks at 1460 cm^{-1} and 1374 cm^{-1}, characteristic of the methylene backbone of the polymer (—CH2—CH). However, the polymer showed a strong peak at 1650–1660 cm^{-1}, corresponding to the carbonyl group within the pyrrolidine ring (Yildiz et al., 2018). Upon complexation, a reduction in the intensity of the bands at 1253 cm^{-1}, 1502 cm^{-1}, and 2922 cm^{-1} was observed, indicating the entrapment of the carbazole structure into the cavity of HPγCD during inclusion complexation. Furthermore, the disappearance of the peak corresponding to the carbonyl group at 1650–1660 cm^{-1} for PVP in the ternary complex suggested that the carbonyl group on the pyrrolidone was involved in forming hydrogen bonds with the outer surfaces of the carvedilol-HPγCD complexes. It is worth noting that the N—H and O—H stretching bands were still present in the complexes, indicating that the mid-section of the carvedilol molecule containing these moieties was not incorporated into the cavity of HPγCD, as illustrated in Fig. 1(D). It is postulated that the exposed amine and hydroxyl groups of carvedilol within the complex, along with the hydroxyl group on the outer surface of HPγCD, may form hydrogen bonds with water molecules when exposed to an aqueous environment, leading to enhanced drug solubility, as observed in Fig. 1(B).

SEM imaging was used to observe the morphology and structure of the complexes at a micron level. Pure carvedilol particles were seen as irregular crystalline rods, while HPγCD and PVP particles appeared as porous spheres, as shown in Fig. 3(F). Binary and ternary physical mixtures of the drug and excipients showed the presence of separate entities without any incorporation, as confirmed by XRD and DSC analysis. After complexation, there was no distinguishable separation between the particles, indicating the formation of either a binary or ternary CD complexation. This, along with DSC and XRD data, suggests the formation of an amorphous CD complex.

NMR spectroscopy was used to investigate carvedilol and HPγCD complexation. H-3 and H-5 protons in the annulus of HPγCD were monitored to determine the level of complexation, as shown in Figs. 4 and S1. Carvedilol forming a complex with CD resulted in a greater degree of Δδ for H-3 and H-5 compared to the physical mixture. The addition of PVP during complexation increased the level of complexation, as shown by greater Δδ for H-3 and H-5. Monitoring H-8 proton, which is located on the outer surface of HPγCD, showed increased proton deshielding with increasing PVP concentration, indicating greater H-bonding between PVP and CD. Carvedilol was successfully incorporated into the cavity of HPγCD, forming a ternary complex with PVP. These ternary complexes were then used to fabricate the needle layer of the dissolving MAPs.

3.3. Fabrication and characterisation of dissolving MAPs

In the current work, a two-step fabrication procedure was employed to fabricate MAP that are loaded carvedilol/CD complexes within the needle layer. It can be seen from Fig. 5(A)–(F), the optical microscopy and SEM images for all five different MAP formulations that are loaded with the carvedilol/CD complexes. All the MAPs appeared transparent on a flat pale base plate as observed from the optical microscope images shown below. On the other hand, the SEM images also showed that MAPs consisted of sharp and clear obelisk projection post fabrication.

The fabricated MAPs were then evaluated for its' mechanical properties and capability to puncture and penetrate the skin. As shown in Fig. 5(F), there is a general trend that with increasing PVP concentration, 0–2.0 %, there is a decrease in the overall percentage of needle height reduction. Nevertheless, such changes in the mechanical property of the needle towards a compressive force of 32 N was not statistically

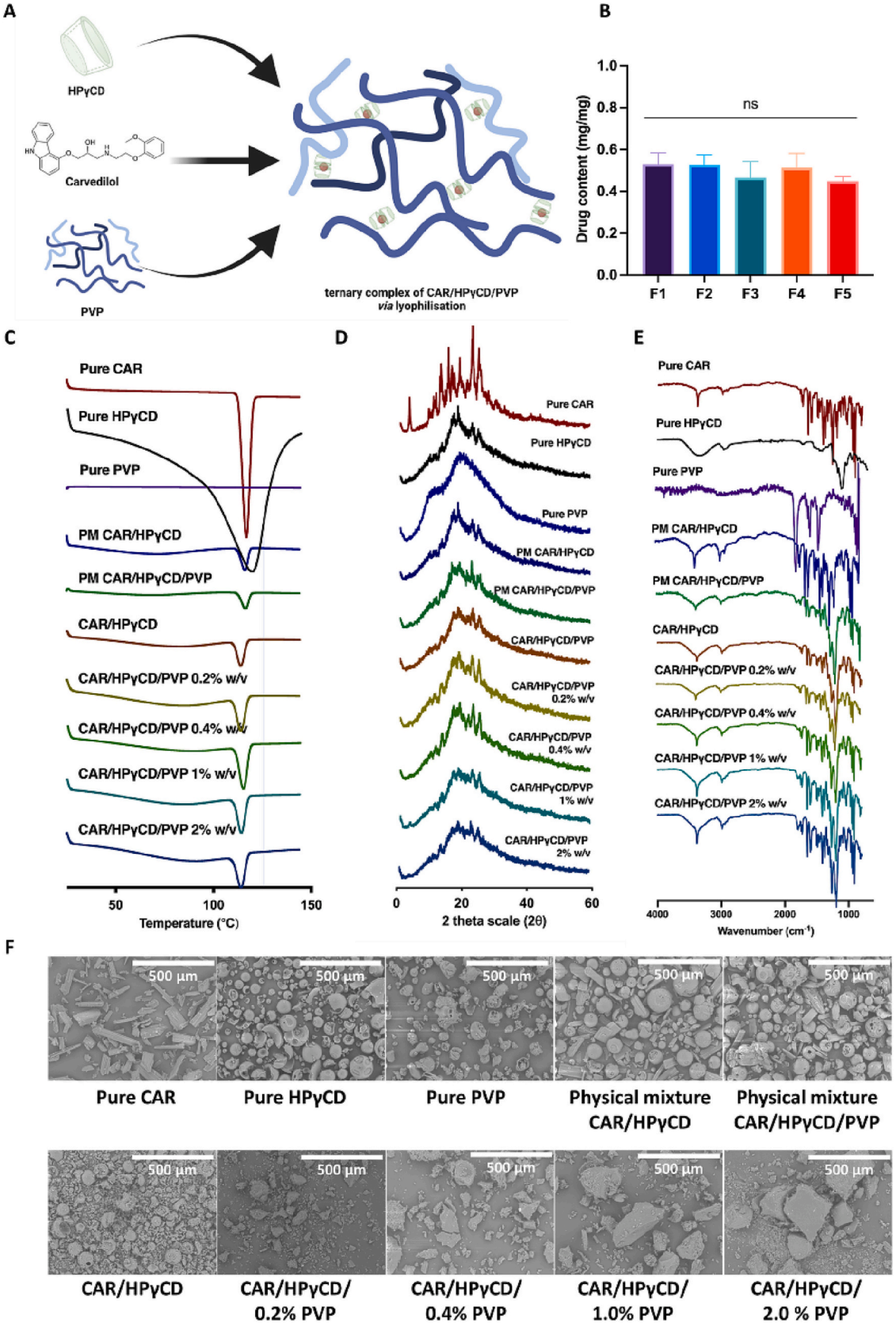

Fig. 3. (A) Formation of carvedilol/HPγCD/PVP ternary complex *via* lyophilisation. Characterisation of carvedilol (CAR): (B) drug content from 1 mg of ternary complex with increasing PVP concentration in F1–F5 (0, 0.2, 0.4, 1.0, 2.0 % *w/v* PVP), (C) DSC thermograms, (D) XRD diffractograms, (E) FTIR spectra and (F) SEM images of pure CAR, pure excipients, physical mixture, binary and ternary complex of the API.

A

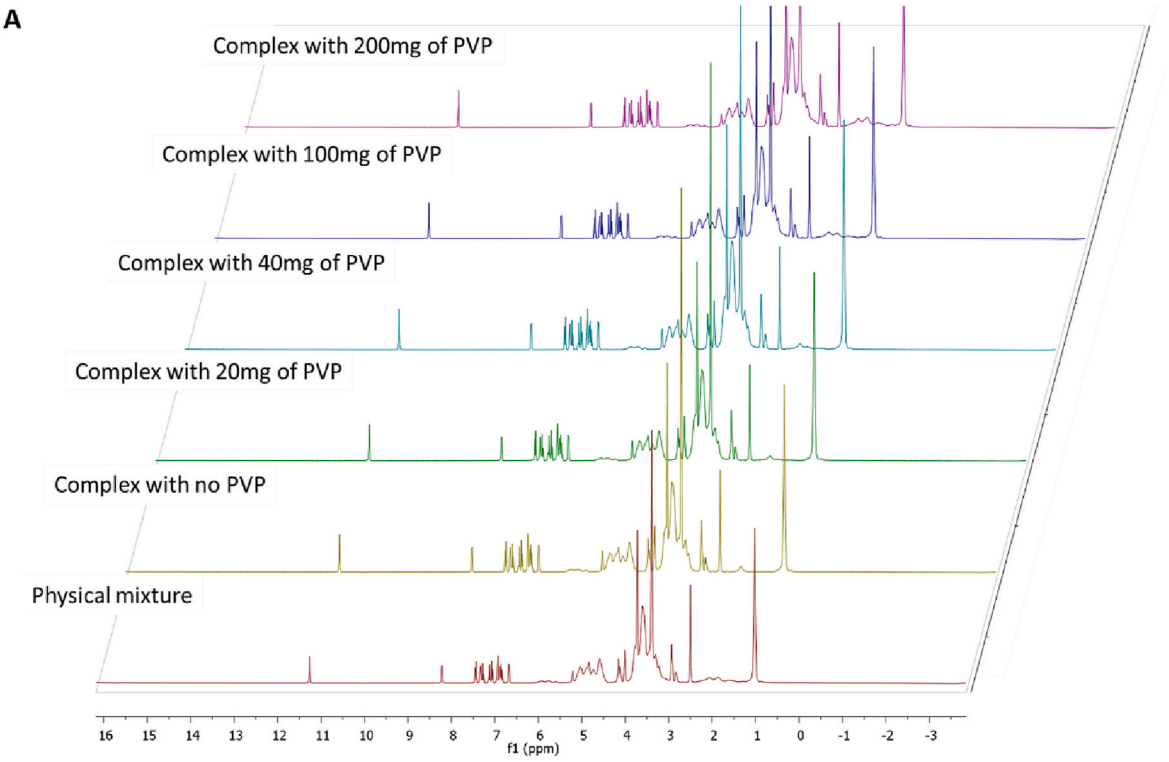

B

Δδ/ppm	Physical Mixture	Complex	Complex + 20 mg of PVP	Complex + 40 mg of PVP	Complex + 100 mg of PVP	Complex + 200 mg of PVP
H-1	0.016	0.016	0.019	0.016	0.016	0.015
H-2	0.007	0.009	0.010	0.011	0.011	0.011
H-3	0.007	0.009	0.013	0.011	0.011	0.011
H-4	0.009	0.01	0.014	0.012	0.012	0.012
H-5	-0.002	0.003	0.007	0.007	0.008	0.014
H-8	0.01	0.01	0.011	0.012	0.012	0.014

Fig. 4. Proton nuclear magnetic resonance (^{1}H NMR) spectra of physical mixtures and complexation powder formed, (B) 1H NMR chemical shift (Δδ) data of HP-γ-CD and the carvedilol complexes. $\Delta\delta = \delta$ (complex) $- \delta$ (free). Peak assignment for ^{1}H NMR is shown in Fig. S1.

significant ($p > 0.05$). In addition, all the manufactured MAP formulations displayed an overall needle height reduction of <10 %. Based on the findings previously published (Anjani et al., 2022c; Kurnia et al., 2022), this suggests the MAP fabricated possess the sufficient mechanical strength needed to withstand the compressive force that is typically exerted during application thus enabling penetration into the skin.

The ability of the patch to puncture the skin was first evaluated *in vitro* using a skin simulant that consisted of eight layers of Parafilm®M. Fig. 5(G) shows the insertion profile of all five carvedilol/CD loaded MAPs across the Parafilm®M layers. In general, all the formulations showed that a majority of the needle shaft penetrated all the way down to third layer of the Parafilm®M stack. This penetration depth equates to ≈350 μm, which is approximately 35 % of the overall needle length. This result is similar to those reported in the literature with similar MAP geometry and design (Anjani et al., 2022e; Permana et al., 2020). It should be noted that the MAP formulations penetrated the first layer of Parafilm®M with 100 % efficiency as evidenced by the any error bars. This would suggest that the MAP would be able to puncture the outermost protective layer of the skin, the *stratum corneum*, with ease enabling the deposition of the drug loaded needle tip into the viable layers of the skin.

The drug loading per patch for each MAP formulation was also evaluated. As shown in Fig. 5(H) the drug loading per patch was ≈1.3–1.5 mg for all five formulations which have a patch size of 0.36 cm^2. From the results it is apparent that the incorporation of PVP into the needle tip composition did have a statistically significant ($p < 0.05$) on the drug loading of the patch. It should be noted that in the management of symptomatic chronic heart failure, patients are given a starting dose of 3.125 mg twice daily which is then increased to 6.25 mg twice daily after which the dose is increased further to 12.5 mg twice daily (Carvedilol | Drugs | BNF | NICE, n.d.). Ultimately, the patients are maintained on a dose 25 mg twice daily. Therefore, based on the drug loading achieved and the established clinical dose regime, it could be postulated that the administration of four MAP patches developed in the current work would provide an equivalent starting daily dose for carvedilol treatment. However, for the subsequent dose, the number of patches that needs to be applied would be too much. In this instance, increasing the patch size may serve as a viable strategy to limit the

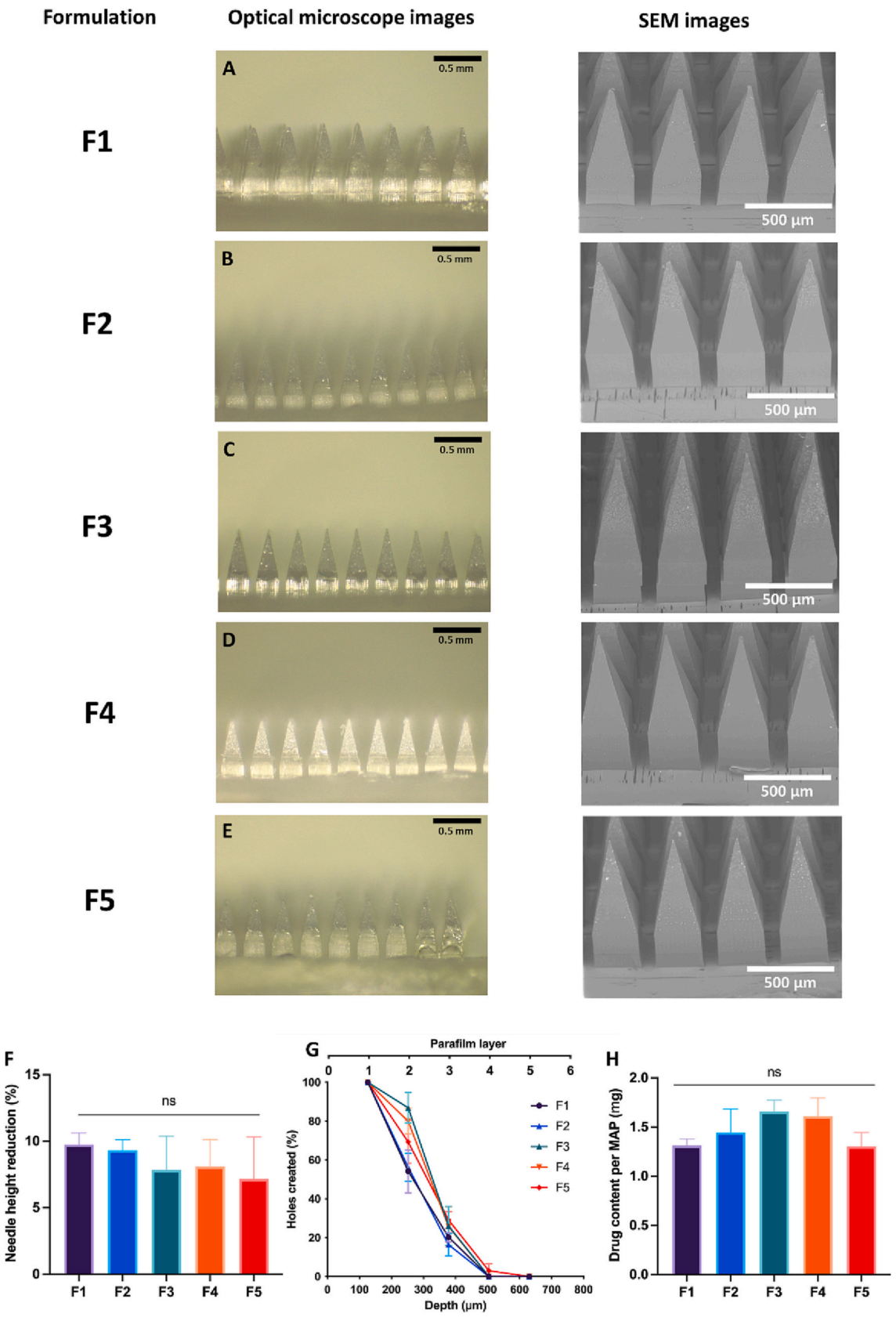

Fig. 5. (A)–(E) Optical microscopy and scanning electron microscopy (SEM) images of different MAPs that are tip prepared with carvedilol/CD complexes. (F) Needle height reduction (%) for MAP loaded with CD-complexes upon being compressed with a 32 N force for 30 s (means + SD, $n = 20$). (G) Percentage of microneedle pores generated per Parafilm® M layer following the insertion of carvedilol/CD loaded MAPs (means ± SD, $n = 3$). (H) Drug content of carvedilol/CD loaded MAPs (means ± SD, n = 3).

number of patches that needs to be administered. It is estimated if the patch size was increased from 0.36 cm^2 to 3.00 cm^2, which is approximately the size of a postage stamp, this would enable us to achieve a drug loading of 12.5 mg per patch. In this instance, the number of patches needed to be applied for the dose escalation would only need to be one patch, followed by two patches before being maintained on daily administration of four patches.

It has been suggested in Fig. 5(F) that the fabricated MAP possesses sufficient mechanical strength needed to puncture the skin. In order to ascertain this, a series of insertion studies involving the application of MAP into the skin simulant, Parafilm®M and *ex vivo* neonatal porcine skin was conducted as shown in Fig. 6(A)–(B). Following MAP application into both *in vitro* and *ex vivo* skin model, the insertion depth of the needle layer was visualised and measured using OCT as shown in Fig. 6(C)–(D). It can be seen from Fig. 6(E), the overall insertion depth of all five MAP formulations into the Parafilm®M layers reached a depth of ≈350 μm. On the other hand, when the patches were applied on *ex vivo* skin, the needles were able to reach an insertion depth of ≈600 μm. It is apparent that the insertion depth of the MAPs into the *ex vivo* skin was deeper than the Parafilm®M layer, an observation that echoes with the findings that we previously reported (Anjani et al., 2022c; Anjani et al., 2022e; Kurnia et al., 2022). The greater MAP insertion depth into *ex vivo* skin relative to Parafilm®M is attributed to presence of interstitial fluid in the *ex vivo* skin, that provide a degree of lubrication that aid the

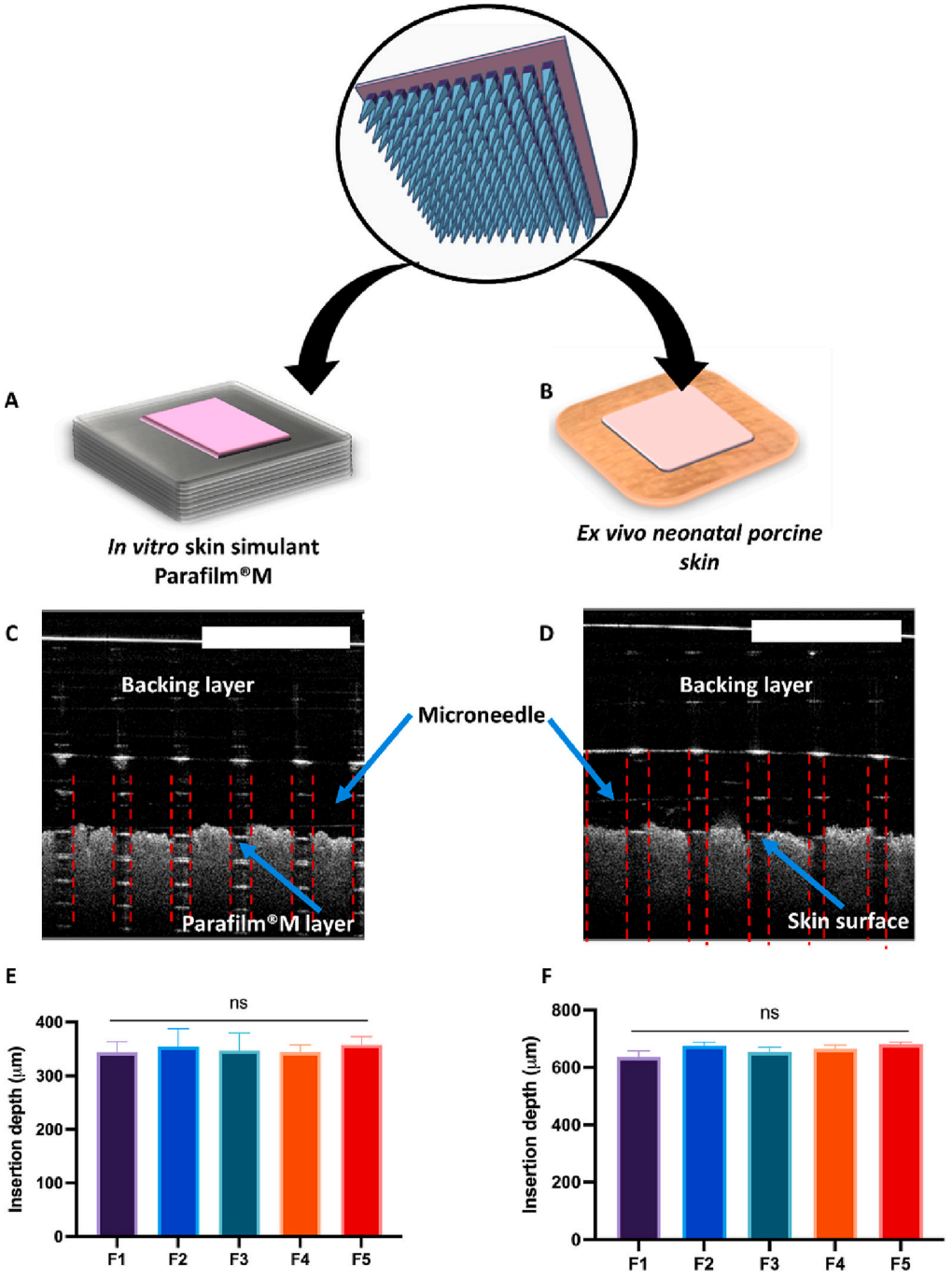

Fig. 6. Characterisation of MAP insertion *via* (A) *in vitro* skin simulant, Parafilm®M, (B) *ex vivo* neonatal porcine skin. Optical coherence tomography (OCT) image of MAP insertion (C) Parafilm®M and (D) *ex vivo* neonatal porcine skin. (E) MAP insertion depth into (E) Parafilm®M and (F) *ex vivo* skin as measured *via* OCT. Data are expressed as means + SD, $n = 20$.

penetration of the needle deeper into the skin relative to Parafilm®M. It can be seen from the skin penetration data that approximately, 70 % of the needle length could be inserted into the skin. This incomplete insertion of the overall needle length is attributed to a combination elasticity of the skin in combination with the 'bed of nail' which may impose some resistance against the complete insertion of the obelisk MAP tip into the skin (Zhang et al., 2018).

One of the cardinal features of dissolving MAPs relative to other categories of MAPs, is the ability of the needle to dissolve and delivery payload upon puncturing the skin. Thus, following the MAP insertion study, we proceed to conduct *in situ* MAP dissolution study to ascertain on the time needed for the needles to dissolves from the baseplate following patch application. It can be seen from Fig. 7, following 30 min of MAP application into *ex vivo* neonatal porcine skin, we observed for all five formulations that most of the needle length have fully dissolved and are embedded in the skin. However, it can be seen that increasing the PVP content within the needle tip from 0 to 2.0 % from F1 to F5, results in less needle dissolution following skin insertion within the first 30 min. This observation may be attributed to the increase in solid content within the needle tips following the addition of PVP, which results in slower needle tip dissolution.

However, when the MAPs were applied for up to 1 h, we observed that the overall needle length for F1 and F2 was completely dissolved, while some needle tip still remained for formulation F3, F4 and F5. However, it was apparent that after 2 h of skin application, all MAP formulations have fully dissolved within the skin resulting in the implantation of the carvedilol/CD loaded tip into the skin. The implanted tip into the skin can be seen from the off-white specks that are formed on the skin which mirrors the needle arrangement on the MAPs. It should be noted, despite carvedilol being a hydrophobic drug, we managed to achieve complete needle dissolution upon skin application. This dissolution can be attributed to incorporation of the hydrophobic drug into the CD cavity. This results in the hydrophobic portion of the drug from being exposed to the dermal interstitial fluid upon skin insertion. Instead, the hydrophilic portion of the CD is capable of forming hydrogen bonds with the water molecules within the dermis resulting in needle dissolution and drug deposition into the skin following application (Wenz, 2012).

3.4. *In vitro permeation study*

An *in vitro* permeation study, as illustrated in Fig. 8(A) was conducted in tandem with the skin dissolution study to investigate the permeation profile of carvedilol into and across the skin following MAP application. Following a 24-h skin application, the amount of drug deposited into the skin is shown in Fig. 8(B). Based on the result, it was apparent that increasing in the concentration of PVP from (0–1.0 % *w/v*) when fabricating the ternary complex within the needle layer of the MAP did not impact the overall drug deposition into the skin ($p > 0.05$). However, when the concentration of PVP used was increased to 2.0 % w/v, we observed a statistically significant ($p < 0.05$) increased in the amount of drug deposited into the skin. This increased in drug deposition into the skin also is also reflected in the amount of drug permeated across the skin as shown in Fig. 8(C). It can also be seen that a majority of the dose of the formulation has been delivered transdermally across the skin over the course of 24 h with some of the dose remain within the skin.

By comparing the skin dissolution data with the permeation data obtained, it can be deduced that, following a 2-h application period, the needle has dissolved and deposited into the skin, leading to the to the formation of micro implants with the skin which continues to release the drug over the course of 24 h, as illustrated in Fig. 8(D). In our previous work, we have shown that by formulating the drug containing layer *via* the addition of only water-soluble polymers (PVP and PVA) resulted in a majority of the dose administered to be deposited into the skin with minimal permeation across the skin (Anjani et al., 2022d). In this instance, we observed that without modifying the drug *via* CD complexation, the hydrophobic nature of carvedilol would cause the drug to remain deposited within the skin while retarding the transdermal permeation profile of the drug. This would result in the

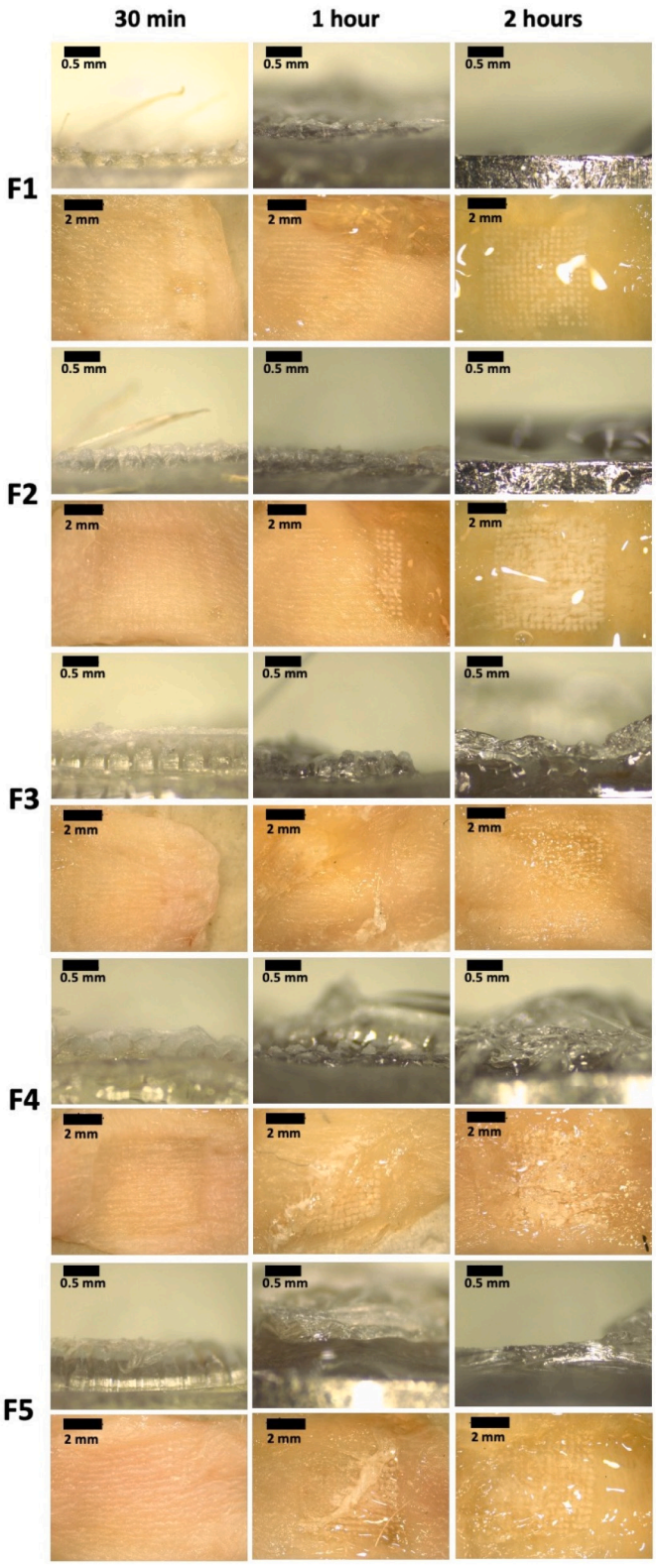

Fig. 7. Digital microscope images of MAP formulation and skin appearance at 30 min, 1 h and 2 h following insertion into excised neonatal porcine skin *ex vivo*.

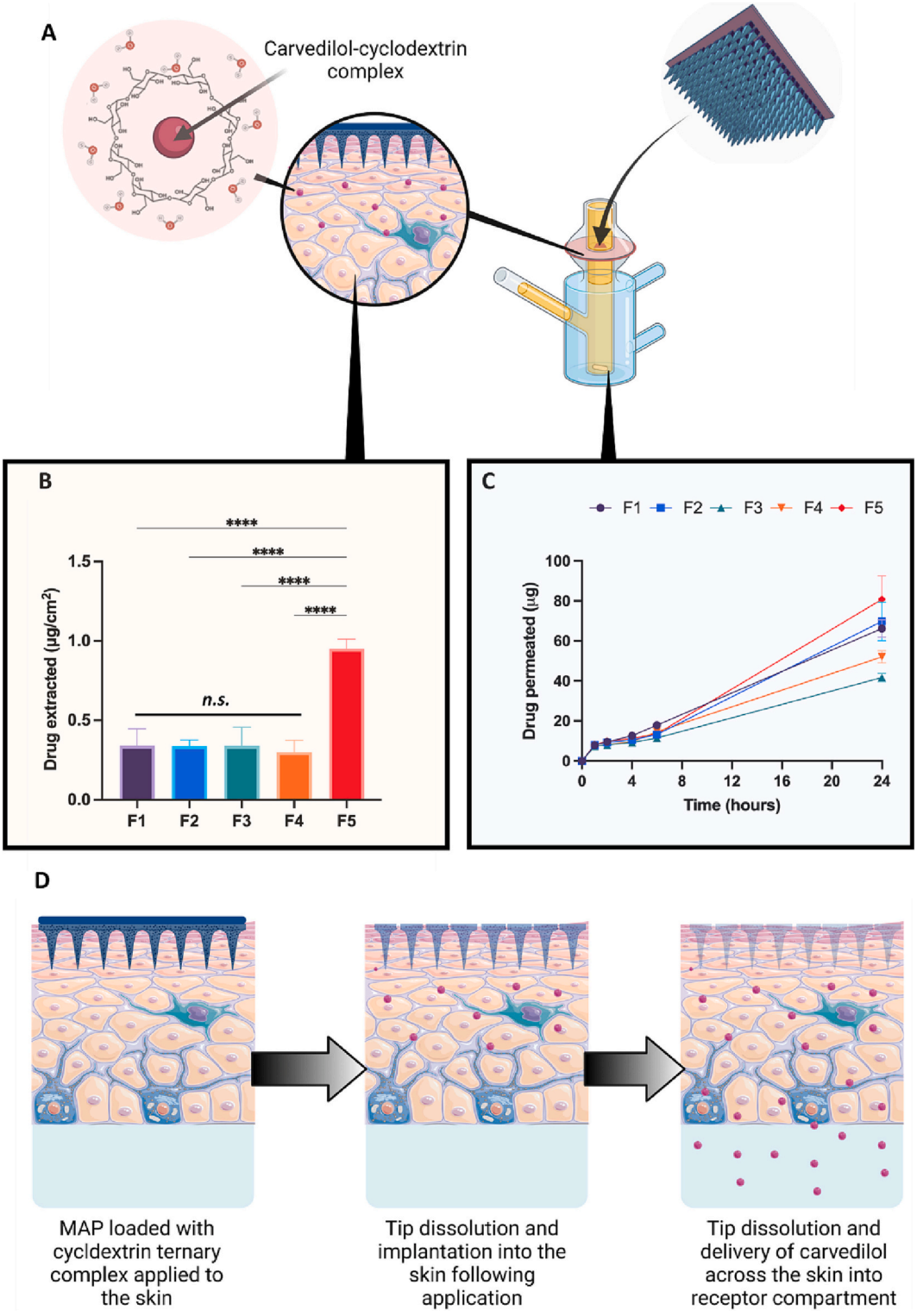

Fig. 8. (A) Schematic illustrating the Franz cell setup to investigate the permeation profile of carvedilol from dissolving MAPs. (B) Amount of carvedilol extracted from the skin and (C) amount of drug permeated across the skin of the Franz cell following 24 h permeation study. Data are expressed as means ± SD, $n = 3$. (D) Schematic illustrating the proposed delivery mechanism of carvedilol across the skin.

formulation being unsuitable for the management of chronic heart failure as we would require a majority of the administered dose to be deliver across the skin to exert its effect systemically. In this work, we have shown that we could increase the hydrophilicity of carvedilol *via* CD complexation that resulted in improved transdermal permeation of the β-blocker.

One of the earliest works that investigated the development of a transdermal patch for the delivery of carvedilol was pioneered by Tanwar et al. (2007). In this early work, Tanwar and coworkers developed HPMC-based drug reservoir that were loaded with Span 80, as a permeation enhancer. In addition, the patches also incorporated Eudragit RS100 and Eudragit RL100 as a rate controlling polymeric

membrane. The researcher demonstrated sustained delivery of the drug over the course of 24 h across guinea pig skin *in vitro* resulting in delivery efficiency of 60–80 % (Tanwar et al., 2007). The delivery efficiency achieved by Tanwar and coworker was significantly higher than that achieved in the current work. Such high delivery efficiency achieved in their early work may be attributed to difference in the skin model used to evaluate the permeation profile of carvedilol *in vitro*. Tanwar and coworkers opted to use guinea pig skin which is far thinner than full thickness human and porcine skin (Todo, 2017). Such physiological discrepancies would ultimately reduce the overall permeation pathway that the drug need to traverse leading to an overall higher delivery efficiency.

Furthering this, Alkilani et al. (Zaid Alkilani et al., 2018) also investigated the utility of using nanoemulsion-based film as a potential transdermal delivery strategy for carvedilol. The carvedilol-loaded nanoemulsion was fabricated from Polysorbate 20, Transcutol®P and oleic acid. Upon optimising the nanoemulsion, the investigator loaded the emulsion into a polymer blend containing HPLMC, chitosan and isopropanol to develop a transdermal patch. Following formulation development, *in vitro* permeation study was performed using Franz cell apparatus to study the permeation profile of carvedilol from the nanoemulsion based patch. Similar to Tanwar et al., the investigator did not use neonatal porcine skin to evaluate the transdermal permeation of carvedilol. Instead, the investigator employed a synthetic membrane Strat-M™ as skin simulant to evaluate the permeation profile of carvedilol. It was discovered that the formulation resulted in a transdermal delivery efficiency of 40 % when the patch was applied over a course of 7 h (Zaid Alkilani et al., 2018). In comparison to the current work, the utilisation of the HPMC-based drug reservoir and nanoemulsion-based film for the transdermal delivery of carvedilol necessitate an extended application period (7–24 h) to achieve a significant transdermal delivery efficiency. Such prolonged skin application may not be acceptable for some patient as this may affect their daily routine as well as increase the propensity of inducing irritation at the site of application (Escobar-Chavez et al., 2012). Therefore, there is an impetus to reduce the duration of application where possible to improve patient compliance while still offering the benefit of transdermal-based drug delivery systems. With our current MAP formulation, we have shown that an application period of up to 2 h was sufficient to enable complete needle dissolution into the skin. The implanted needle tip was then able to form depot that was able to deliver the drug transdermally across the skin. This reduced application time may be well suited for patients as they can apply it discretely for a short period of time without affecting their daily routine. In contrast to the work by Tanwar et al. and Alkilani et al., the development of dissolving MAPs for the delivery of carvedilol did not employ the use of any surfactants to enhance the transdermal permeation of the β-blocker. The absence of any surfactant within the dissolving MAP helps to mitigate the likelihood of inducing any skin irritation upon patch application, which is typically associated with the use of surfactant (Kreilgaard, 2002).

3.5. Biocompatibility study

After conducting an *in vitro* permeation study, it was found that formulation F5 was the most effective at delivering carvedilol through the skin. The biocompatibility of this formulation with dermal cells was then examined. The results of our investigation, depicted in Fig. 10(A), showed that the carvedilol/CD/PVP loaded dissolving MAPs and CD/PVP loaded dissolving MAPs did not affect cell viability after 72 h, with no significant changes compared to the control ($p > 0.05$). This was confirmed by the results of the live and dead staining (Fig. 9(B)), which showed no dead cells. The fibroblast proliferation was also evaluated using the PicoGreen assay (Fig. 9(C)), and the results indicated that neither formulation had a significant effect on the proliferation potential of the fibroblasts ($p > 0.05$). These findings support the idea that the exposure of the cells to the formulation did not affect their viability, proliferation potential, or plasma membrane integrity, which may be due to the low amount of drug that can be soluble in DMEM media (264.8 ± 55.32 μg/mL). The literature acknowledges the beneficial effects of carvedilol in low doses and its low probability of affecting skin cells (Chen et al., 2020; Zhang et al., 2021), so from a clinical standpoint, these results suggest that MAP loaded with carvedilol is

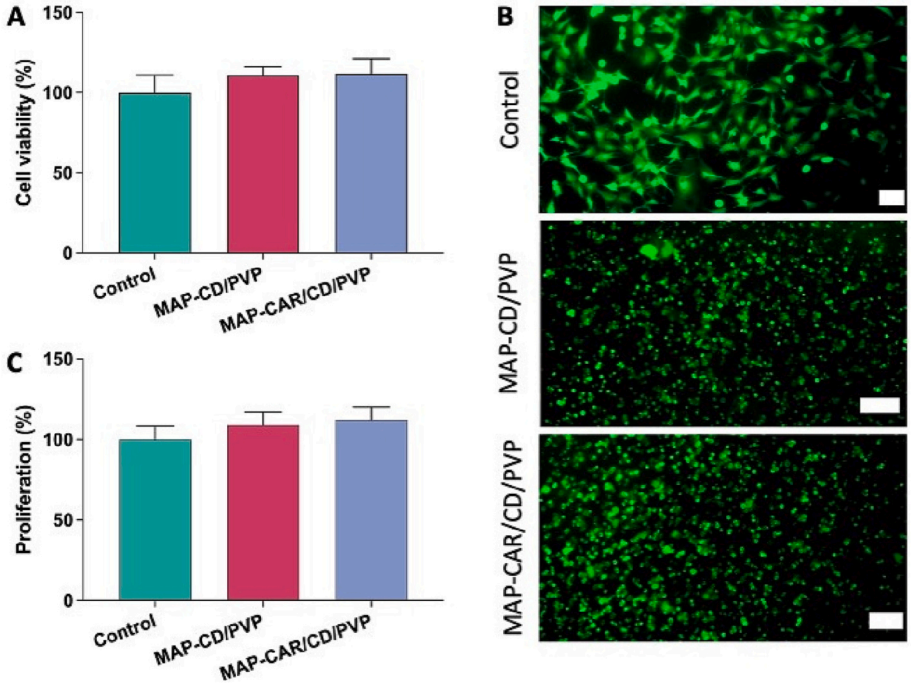

Fig. 9. (A) Percentage of viable cells after a culture period of 72 h. (b) Live/dead staining of fibroblastic cells on control, green represents live cells; scale bar = 100 μm. (C) Total DNA content of cells on control, carvedilol/CD/PVP loaded dissolving MAPs and CD/PVP loaded dissolving MAPs samples cultured for a time period of 72 h. Data points represent means + SD ($n = 3$).

biocompatible and unlikely to be toxic to the skin.

3.6. Pharmacokinetic study

During the *in vivo* study, upon the removal of the MAP after 24 h we observed that the needle layers have completely dissolved. In addition, there were no indications of skin irritation on any of the rats (Fig. S2), post-MAP removal, which corroborates the biocompatibility data shown in Section 3.5. In addition, histological analysis of the liver was also conducted in order to evaluate the potential toxicity of the formulation following administration into the animal. As shown in the supplementary data in Fig. S3, the transdermal administration of carvedilol *via* MAPs did not induce any noticeable signs of hepatotoxicity relative to the oral group as well as the positive and negative control. This data further supports the biocompatibility of the formulation *in vivo*.

The pharmacokinetic profiles of carvedilol following MAP and oral administration is shown in Fig. 10(B). Upon oral administration there was a sharp rise in plasma concentration of carvedilol, which reached a C_{max} of 43.2 ng/mL within 3 h following oral administration as shown in the Table in Fig. 10(C). The T_{max} observed for the oral group in the current work is similar to those previously reported (Mo et al., 2022; Sharma et al., 2019b). However, it should be noted, when carvedilol was administered as a dissolving MAP, we observed a significant shift ($p < 0.05$) in T_{max} from 3 h to 41 h. In addition, we also noticed that the C_{max} increased from 43.2 ng/mL to 59.4 ng/mL, although such increase in C_{max} was not statistically significant ($p > 0.05$). Also worth noting, regardless of the administration route the half-life of carvedilol remained the same, 31.6 h.

The shift in T_{max} following transdermal delivery of carvedilol relative to oral administration has also been observed by other researchers. For instance, Mo et al. (2022) and Ubaidulla et al. (2007) observed that formulating carvedilol into conventional transdermal patches resulted in in a delay in T_{max} from 2 h to 12 h (Mo et al., 2022; Ubaidulla et al., 2007). This delay may arise due to the time taken for the drug to traverse across the different layers of the skin and into the dermal microcirculation which would eventually lead to systemic exposure. However, this delay in T_{max} when carvedilol was delivered using dissolving MAP was far greater than that of conventional transdermal patches. This delay may be attributed to the time taken for the CD complex to dissolve from the implanted needle tips before reaching the systemic circulation, as illustrated in Fig. 8(D). This process would not typically occur for conventional transdermal patches as the drug would passively and continuously diffuses across the skin from the drug loaded layers into dermal microcirculation. It could be postulated that the delay in needle dissolution may account for the greater shift in T_{max} observed. In addition, it can be seen that carvedilol undergoes rapid elimination once absorbed as evidenced from the rapid decrease in plasma concentration of the drug after ≈3 h post oral administration as shown in Fig. 10(B). This indicates that the drug is rapidly metabolised and eliminated from the body when delivered *via* the oral route. However, in the case of CD based dissolving MAPs, we observed a steady increase in plasma concentration following MAP administration. It has also been reported that CD complexation also enhances the stability of the delivered payload by reducing drug metabolism enabling to the payload to circulate for a prolonged period leading to enhanced systemic effect (Kurkov & Loftsson, 2013). Therefore, it is postulated the combination of the time taken for the complex to be released from the needle tip in tandem with the enhanced stability conferred by the complex may lead to a delay in the T_{max} achieved following MAP administration. The enhancement in stability and circulation time of CD within the systemic circulation is also evidenced from the enhancement in mean residence time of carvedilol when the drug was delivered by MAP (55 h) relative to oral administration (31 h).

In addition, we observed that the AUC for MAP treated group was 7-folds higher than that of the oral treatment group. In pharmacokinetics, AUC represents the actual exposure of the animals to carvedilol post

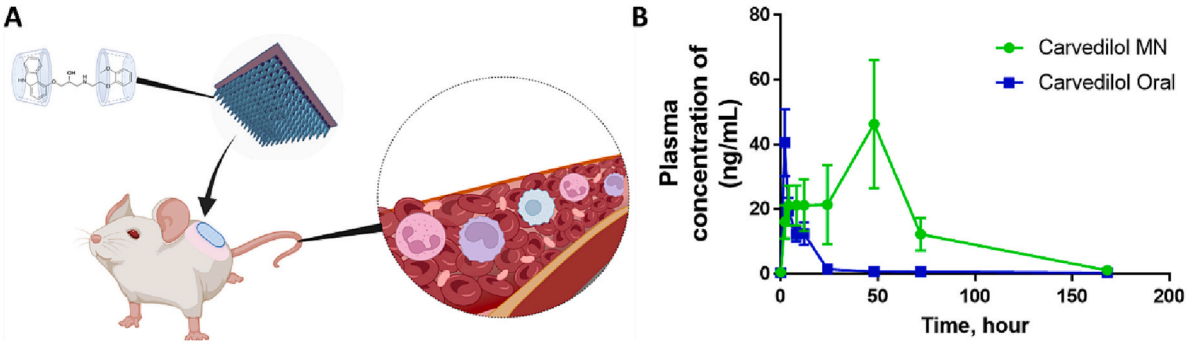

C

Pharmacokinetic Parameters	MAP treatment group	Oral Treatment Group
Area under the concentration-time curve, ***AUC*** (ng.hr mL−1)	2150 ± 480	355 ± 35
Maximum plasma concentration, C_{max} (ng.mL−1)	59.4 ± 18.7	43.2 ± 9.6
Time until C_{max} is reached, T_{max} (hr)	41 ± 9.1	3.0 ± 0.42
Half life, $T_{1/2}$(hr)	31.6 ± 6.4	30.4 ± 6.0
Mean residence time (hr)	55.4 ± 5.9	31.3 ± 3.4

Fig. 10. (A) Schematic illustrating the delivery of carvedilol *in vivo* using dissolving MAPs with CD ternary complex tips. (B) Plasma level of carvedilol over time for rats treated with either dissolving MAPs or oral gavage. (C) Pharmacokinetic parameters, AUC, C_{max}, T_{max} following dose administration. Data are expressed as means ± SEM, $n = 6$.

dose administration. This parameter provides a useful insight on the overall bioavailability of the drug. In this instance, the AUC indicates that delivery of carvedilol *via* dissolving MAP resulted in enhanced bioavailability relative to oral administration. It has been reported that carvedilol exhibit an overall oral bioavailability of 25–35 %. This low oral bioavailability is attributed to the hydrophobicity of the drug coupled with the high first pass metabolism that carvedilol undergoes post absorption (Sharma et al., 2019a). In the current work, we have circumvented these two limitations by first enhancing the hydrophilicity of carvedilol through CD complexation as well as obviating first pass metabolism by delivering the drug directly into systemic circulation *via* the transdermal route. It is postulated that the combination of these drug delivery strategies has augmented the overall bioavailability of carvedilol following MAP administration.

With respect to enhancement in bioavailability following MAP application relative to oral delivery, several researchers have also observed similar trends. For instance, Permana et al. (2019) demonstrated that, by formulating doxycycline, diethylcarbamazine and albendazole into solid lipid nanoparticle-based dissolving MAPs, bioavailability of the drug was enhanced, increased systemic exposure (Permana et al., 2019). Furthering this, Ramadon et al. (2020) also discovered that delivering the antibiotic vancomycin *via* dissolving and hydrogel-forming MAPs led to enhanced bioavailability relative to oral administration (Ramadon et al., 2020). Based on these earlier studies and in light with our recent work, formulating a hydrophobic drug that typically exhibits poor oral absorption into dissolving MAP provide a potential solution to enhance the overall bioavailability of the delivered payload.

Based on the literature and our current formulation data, it could be postulated that the main driving condition by which carvedilol is released from cyclodextrin ternary complexes is mainly *via* simple dilution. Upon skin application, the implanted tip will undergo polymer (PVP) swelling and dissolution which in turn release the secondary HPγCD-carvedilol complex into the skin (Sabri et al., 2020). This secondary complex will then move into systemic circulation where it will undergo significant dilution. As the drug/cyclodextrin complexes are in a constant state of equilibria between complex formation and dissociation, the dilution of the complex in plasma would cause a shift in equilibria promoting complex dissociation. Based on Le Chatelier's principle, this in turn would result in further release of the guest molecule, in this instance carvedilol, into the blood stream. Although it could not be fully ruled out, the potential role of competitive displacement of the guest molecules by endogenous materials as well as the binding of the drug to plasma protein may also aid the release of the drug from the cyclodextrin complex (Stella et al., 1999).

In addition, histological analysis on the lumen diameter of the aorta was also conducted in order to study the vasodilation effect of the formulation on the arteries of the rat as illustrated in Fig. 11(A). It can be seen from Fig. 11(B)–(C) that treatment with either oral administration or *via* dissolving MAP resulted in some level of aorta dilation. However, the dilation achieved by a single oral administration of carvedilol was not significant relative to untreated rats. In contrast, the administration of carvedilol *via* dissolving MAP loaded with CD complexes resulted in a statistically significant ($p < 0.05$) dilation in the aorta relative to both the untreated and oral treatment group. It is known that β-blockers may be classified as either non-vasodilators (*e.g.*, propranolol, atenolol and bisoprolol) or vasodilators (*e.g.*, carvedilol, bucindolol, acebutolol) (Shah et al., 2011). As carvedilol is by virtue both a β-blocker and a vasodilator, the drug manages hypertension *via* significantly decreases myocardial work through reducing heart rate, contractility, and wall tension (Ruffolo & Feuerstein, 1997). The third pharmacological effect of carvedilol is apparent in the current work as rats that were treated

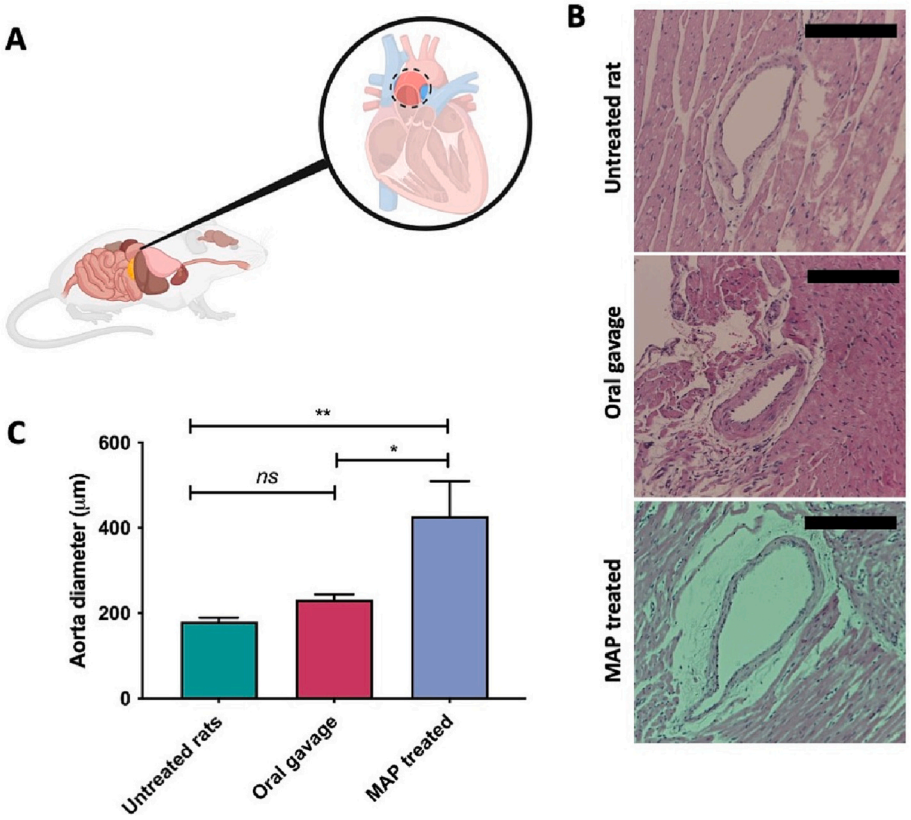

Fig. 11. (A) Schematic illustrating the analysis of the rat aorta following the completion of the pharmacokinetic study in order to study the vasodilation effect of the formulation. (B) Representative histological analysis of the aorta of rats that were untreated or those that were either treated with oral administration of carvedilol or *via* dissolving MAPs. (C) Aorta diameter of rats from different treatment group. Data are expressed mean + SEM, $n = 6$.

orally or *via* dissolving MAP exhibit a decrease in aortic wall tension leading to the widening of the aortic lumen. However, this vasodilatory effect was only significant when the drug was delivered *via* CD complex using dissolving MAP. This may be attributed to the longer systemic circulation time of carvedilol in the rat when the drug is delivered using dissolving MAP as evidenced by the longer mean residence time relative to oral administration. This longer residence time, enable the drug to result in prolonged blockade of arterial α1-adrenoceptors, thereby culminate in vasodilation (Feuerstein & Ruffolo, 1996). This will ultimately result in a maintenance to the stroke volume and cardiac output in patients with congestive heart failure who are treated with carvedilol.

Based on the plasma level of carvedilol, as shown in Fig. 10(B), along with vasodilatory effect exhibited in Fig. 11(C), we observed that utilising dissolving MAPs provide a potential solution to sustain the delivery of carvedilol for up to several days following a single patch application. From a clinical standpoint, this would suggest that using CD-based dissolving MAP may provide a convenient way to deliver the β-blocker in a sustain fashion with less frequent dosing relative to oral administration. Currently, carvedilol is administered as oral tablet at a dose of 50 mg daily. Based on our proof-of-concept work, by formulating the drug into a CD based dissolving MAP, we could potentially reduce the dosing frequency of the drug down to twice a week. In addition, with the rapid tip dissolution, the patient would only need to apply the patch for up to 2 h in order to implant the drug loaded tip into the skin, which would then form a CD depot that releases the drug in a sustain fashion for over several days.

Overall, reformulating carvedilol into a ternary complex *via* dissolving MAPs offer a potential approach to revolutionise the way we manage and treat heart failure. Nevertheless, considerable effort should still be made in order to translate this technology into clinical practice. For instance, in order to promote the translation of this technology into clinical use, formulators and engineers ought to work closely with end users, in this instance the patient, in order to identify any additional human factors that ought to be considered when designing the overall product. For examples, it would be judicious to develop an applicator that could aid in the administration of the patch in a reproducible and consistent fashion between patients. In doing so, this would aid in minimising dosing variability between patients while ensuring the patients are receiving the right dose following every patch administration. In addition, formulators and researchers ought to be engaging with clinicians and the general public in order to promote the technology further. Currently, there is a lacuna between the public awareness of the potential emerging pharmaceutical technologies with the progress and advancement within the field. By actively engaging with end users (*e.g.*, through public outreach events), researcher may help promote the clinical utility of MAPs to the public which will help generate a strong market demand for the technology. In doing so, this will spike interest among industrial partners in bringing the technology forward towards commercialisation.

4. Conclusion

In this study, we successfully formed inclusion ternary complexes of carvedilol/HPγCD/PVP and fabricated them into water-soluble needle tips. PVP was chosen as the polymer for the ternary inclusion complex in the MAP fabrication process due to its ability to significantly increase the solubility of carvedilol/HPγCD complexes compared to PVA, with a 1.7-fold higher solubility. Permeation studies using full-thickness *ex vivo* neonatal porcine skin demonstrated that MAPs loaded with the ternary complex could effectively deliver the drug transdermally. Additionally, in a pharmacokinetic study conducted on rats, it was observed that MAPs with carvedilol/HPγCD/PVP tips achieved substantially higher and more sustained plasma levels of carvedilol compared to oral administration over a period of seven days. If this CD-based dissolving MAP is translated into clinical practice, it has the potential to significantly reduce the pill burden in individuals with symptomatic chronic heart failure.

Funding

This study was supported by The Wellcome Trust with grant number WT094085MA.

CRediT authorship contribution statement

Qonita Kurnia Anjani: Conceptualization, Methodology, Visualization, Investigation, Validation, Formal analysis, Data curation, Writing – original draft, Writing – review & editing. **Akmal Hidayat Bin Sabri:** Visualization, Investigation, Formal analysis, Writing – original draft. **Khuriah Abdul Hamid:** Methodology, Formal analysis, Data curation, Investigation. **Natalia Moreno-Castellanos:** Methodology, Formal analysis, Data curation, Investigation. **Huanhuan Li:** Methodology, Investigation. **Ryan F. Donnelly:** Resources, Writing – review & editing, Supervision, Funding acquisition.

Declaration of competing interest

The authors declare no competing interest.

Data availability

The data is available from the corresponding author upon request.

Appendix A. Supplementary data

Supplementary data to this article can be found online at https://doi.org/10.1016/j.carbpol.2023.121194.

References

Anjani, Q. K., Bin Sabri, A. H., Domínguez-Robles, J., Moreno-Castellanos, N., Utomo, E., Wardoyo, L. A. H., Larrañeta, E., & Donnelly, R. F. (2022a). Metronidazole nanosuspension loaded dissolving microarray patches: An engineered composite pharmaceutical system for the treatment of skin and soft tissue infection. *Biomaterials Advances, 140*, Article 213073. https://doi.org/10.1016/J.BIOADV.2022.213073

Anjani, Q. K., Bin Sabri, A. H., McGuckin, M. B., Li, H., Hamid, K. A., & Donnelly, R. F. (2022d). In Vitro permeation studies on carvedilol containing dissolving microarray patches quantified using a rapid and simple HPLC-UV analytical method. *AAPS PharmSciTech, 23*. https://doi.org/10.1208/s12249-022-02422-6

Anjani, Q. K., Bin Sabri, A. H., Utomo, E., Domínguez-Robles, J., & Donnelly, R. F. (2022). Elucidating the impact of surfactants on the performance of dissolving microneedle array patches. *Molecular Pharmaceutics*. https://doi.org/10.1021/acs.molpharmaceut.1c00988

Anjani, Q. K., Domínguez-Robles, J., Utomo, E., Font, M., Martínez-Ohárriz, M. C., Permana, A. D., Cárcamo-Martínez, Á., Larrañeta, E., & Donnelly, R. F. (2021a). Inclusion complexes of rifampicin with native and derivatized cyclodextrins. In *, 15. Silico modeling, formulation, and characterization, pharmaceuticals (basel)*. https://doi.org/10.3390/PH15010020

Anjani, Q. K., Domínguez-Robles, J., Utomo, E., Font, M., Martínez-Ohárriz, M. C., Permana, A. D., Cárcamo-Martínez, Á., Larrañeta, E., & Donnelly, R. F. (2022f). Inclusion complexes of rifampicin with native and derivatized cyclodextrins: In silico modeling, formulation, and characterization. *Pharmaceuticals., 15*. https://doi.org/10.3390/ph15010020

Anjani, Q. K., Hidayat, A., Sabri, B., Moreno-Castellanos, N., Utomo, E., Cárcamo-Martínez, Á., … Donnelly, R. F. (2022b). Soluplus®-based dissolving microarray patches loaded with colchicine: Towards a minimally invasive treatment and management of gout. *Biomaterials Science*. https://doi.org/10.1039/D2BM01068B

Anjani, Q. K., Hidayat, A., Sabri, B., Moreno-castellanos, N., Utomo, E., Cárcamo-martínez, Á., … Donnelly, R. F. (2022c). Soluplus®-based dissolving microarray patches loaded with colchicine: Towards a minimally invasive treatment and management of gout. *Biomaterials Science*. https://doi.org/10.1039/d2bm01068b

Anjani, Q. K., Permana, A. D., Cárcamo-Martínez, Á., Domínguez-Robles, J., Tekko, I. A., Larrañeta, E., Vora, L. K., Ramadon, D., & Donnelly, R. F. (2021b). Versatility of hydrogel-forming microneedles in in vitro transdermal delivery of tuberculosis drugs. *European Journal of Pharmaceutics and Biopharmaceutics., 158*, 294–312. https://doi.org/10.1016/j.ejpb.2020.12.003

Bejaoui, M., Galai, H., Amara, A. B. H., & Ben Rhaiem, H. (2019). Formation of water soluble and stable amorphous ternary system: Ibuprofen/β-cyclodextrin/PVP. *Glass Physics and Chemistry., 45*, 580–588. https://doi.org/10.1134/S1087659619060130

Carvedilol | Drugs | BNF | NICE. n.d. https://bnf.nice.org.uk/drugs/carvedilol/. (Accessed 7 February 2023)

Chen, M., Shamim, M. A., Shahid, A., Yeung, S., Andresen, B. T., Wang, J., Nekkanti, V., Meyskens, F. L., Kelly, K. M., & Huang, Y. (2020). Topical delivery of carvedilol loaded nano-transfersomes for skin cancer chemoprevention. *Pharmaceutics, 12*, 1151, 12 (2020) 1151 https://doi.org/10.3390/PHARMACEUTICS12121151.

Do Vale, G., Ceron, C. S., Ginzaga, N., Simplicio, J. A., & Padovan, J. (2019). Three generations of β-blockers: History, class differences and clinical applicability. *Current Hypertension Reviews*, 22–31. https://doi.org/10.2174/1573402114666180918102735

Dodson, J. A., & Chaudhry, S. I. (2012). Geriatric conditions in heart failure. *Current Cardiovascular Risk Reports, 6*, 404–410. https://doi.org/10.1007/s12170-012-0259-8

Eichhorn, E. J., & Bristow, M. R. (2001). The carvedilol prospective randomized cumulative survival (COPERNICUS) trial. *Current Controlled Trials in Cardiovascular Medicine, 2*, 20–23. https://doi.org/10.1186/CVM-2-1-020

Escobar-Chavez, J., Diaz-Torres, R., Rodriguez-Cruz, I. M., Dominguez-Delgado, Sampere-Morales, Angeles-Anguiano, & Melgoza-Contreras. (2012). Nanocarriers for transdermal drug delivery. *Research and Reports in Transdermal Drug Delivery, 3*. https://doi.org/10.2147/rrtd.s32621

Feuerstein, G. Z., & Ruffolo, R. R. (1996). Carvedilol, a novel vasodilating beta-blocker with the potential for cardiovascular organ protection. *European Heart Journal, 17*, 24–29. https://doi.org/10.1093/eurheartj/17.suppl_b.24

Grogan, M., & Dispenzieri, A. (2015). Natural history and therapy of AL cardiac amyloidosis. *Heart Failure Reviews, 20*, 155–162. https://doi.org/10.1007/s10741-014-9464-5

He, H., Wang, Z., Aikelamu, K., Bai, J., Shen, Q., Gao, X., & Wang, M. (2023). Preparation and in vitro characterization of microneedles containing inclusion complexes loaded with progesterone. *Pharmaceutics, 15*, 1765, 15 (2023) 1765 https://doi.org/10.3390/PHARMACEUTICS15061765.

Higuchi, T., & Connor, K. A. (1965). *Phase solubility techniques* (New York).

Hirlekar, R., & Kadam, V. (2009a). Preparation and characterization of inclusion complexes of carvedilol with methyl-β-cyclodextrin. *Journal of Inclusion Phenomena and Macrocyclic Chemistry, 63*, 219–224. https://doi.org/10.1007/s10847-008-9506-5

Hirlekar, R., & Kadam, V. (2009b). Preparation and characterization of inclusion complexes of carvedilol with methyl-β-cyclodextrin. *Journal of Inclusion Phenomena and Macrocyclic Chemistry, 3–4*, 219–224. https://doi.org/10.1007/S10847-008-9506-5

Investigators, T. C. (2001). Effect of carvedilol on outcome after myocardial infarction in patients with left-ventricular dysfunction: The CAPRICORN randomised trial. *Lancet., 357*, 1385–1390. https://doi.org/10.1016/S0140-6736(00)04560-8

Kim, Y. T., Shin, B. K., Garripelli, V. K., Kim, J. K., Davaa, E., Jo, S., & Park, J. S. (2010). A thermosensitive vaginal gel formulation with HPγCD for the pH-dependent release and solubilization of amphotericin B. *European Journal of Pharmaceutical Sciences., 41*, 399–406. https://doi.org/10.1016/j.ejps.2010.07.009

Kreilgaard, M. (2002). Influence of microemulsions on cutaneous drug delivery. *Advanced Drug Delivery Reviews, 1*. https://doi.org/10.1016/S0169-409X(02)00116-3

Kurkov, S. V., & Loftsson, T. (2013). Cyclodextrins. *International Journal of Pharmaceutics, 453*, 167–180. https://doi.org/10.1016/j.ijpharm.2012.06.055

Kurnia, Q., Hidayat, A., Sabri, B., Domínguez-robles, J., & Donnelly, R. F. (2022). Metronidazole nanosuspension loaded dissolving microarray patches: An engineered composite pharmaceutical system for the treatment of skin and soft tissue infection. *Biomaterials Advances., 140*. https://doi.org/10.1016/j.bioadv.2022.213073

Larrañeta, E., Moore, J., Vicente-Pérez, E. M., González-Vázquez, P., Lutton, R., Woolfson, A. D., & Donnelly, R. F. (2014). A proposed model membrane and test method for microneedle insertion studies. *International Journal of Pharmaceutics, 472*, 65–73. https://doi.org/10.1016/j.ijpharm.2014.05.042

Lin, S., Quan, G., Hou, A., Yang, P., Peng, T., Gu, Y., … Wu, C. (2019). Strategy for hypertrophic scar therapy: Improved delivery of triamcinolone acetonide using mechanically robust tip-concentrated dissolving microneedle array. *Journal of Controlled Release, 306*, 69–82. https://doi.org/10.1016/J.JCONREL.2019.05.038

Loftsson, T., & Brewster, M. E. (2010). Pharmaceutical applications of cyclodextrins: Basic science and product development. *Journal of Pharmacy and Pharmacology., 62*, 1607–1621. https://doi.org/10.1111/J.2042-7158.2010.01030.X

Loftsson, T., Fririksdóttir, H., & Gumundsdóttir, T. K. (1996). The effect of water-soluble polymers on aqueous solubility of drugs. *International Journal of Pharmaceutics, 127*, 293–296. https://doi.org/10.1016/0378-5173(95)04207-5

Loftsson, T., Jarho, P., Másson, M., & Tomi, J. (2005). Cyclodextrins in drug delivery system. *Expert Opinion on Drug Delivery, 2*, 335–351. https://doi.org/10.1517/17425247.2.1.335

Loftsson, T., Vogensen, S. B., Desbos, C., & Jansook, P. (2008a). Carvedilol: Solubilization and cyclodextrin complexation: A technical note. *AAPS PharmSciTech, 9*, 425–430. https://doi.org/10.1208/s12249-008-9055-7

Loftsson, T., Vogensen, S. B., Desbos, C., & Jansook, P. (2008b). Carvedilol: Solubilization and cyclodextrin complexation: A technical note. *AAPS PharmSciTech, 9*, 425. https://doi.org/10.1208/S12249-008-9055-7

Mo, L., Lu, G., Ou, X., & Ouyang, D. (2022). Formulation and development of novel control release transdermal patches of carvedilol to improve bioavailability for the treatment of heart failure, Saudi. *Journal of Biological Sciences, 29*, 266–272. https://doi.org/10.1016/j.sjbs.2021.08.088

Mora, M. J., Petiti, J. P., Longhi, M. R., Torres, A. I., & Granero, G. E. (2015). Intestinal uptake and toxicity evaluation of acetazolamide and its multicomponent complexes with hidroxypropyl-β-cyclodextrin in rats. *International Journal of Pharmaceutics, 478*, 258–267. https://doi.org/10.1016/j.ijpharm.2014.11.027

National Institute for Health and Care Excellence. (2018). *Chronic heart failure in adults: diagnosis and management* (pp. 1–36). NICE Clinical Guideline. https://www.nice.org.uk/guidance/ng106/chapter/Recommendations.

Paria, S., Biswal, N., & Chaudhuri, R. (2012). Surface tension, adsorption, and wetting behaviors of natural surfactants on a PTFE surface. *AIChE Journal., 59*, 215–228. https://doi.org/10.1002/aic.14674

Permana, A. D., Paredes, A. J., Volpe-Zanutto, F., Anjani, Q. K., Utomo, E., & Donnelly, R. F. (2020). Dissolving microneedle-mediated dermal delivery of itraconazole nanocrystals for improved treatment of cutaneous candidiasis. *European Journal of Pharmaceutics and Biopharmaceutics., 154*, 50–61. https://doi.org/10.1016/j.ejpb.2020.06.025

Permana, A. D., Tekko, I. A., McCrudden, M. T. C., Anjani, Q. K., Ramadon, D., McCarthy, H. O., & Donnelly, R. F. (2019). Solid lipid nanoparticle-based dissolving microneedles: A promising intradermal lymph targeting drug delivery system with potential for enhanced treatment of lymphatic filariasis. *Journal of Controlled Release, 316*, 34–52. https://doi.org/10.1016/j.jconrel.2019.10.004

Poole-Wilson, P. A., Swedberg, K., Cleland, J. G. F., Di Lenarda, A., Hanrath, P., Komajda, M., Lubsen, J., Lutiger, B., Metra, M., Remme, W. J., Torp-Pedersen, C., Scherhag, A., & Skene, A. (2003). Comparison of carvedilol and metoprolol on clinical outcomes in patients with chronic heart failure in the Carvedilol Or Metoprolol European Trial (COMET): Randomised controlled trial. *Lancet., 362*, 7–13. https://doi.org/10.1016/S0140-6736(03)13800-7

Prado, L. D., Rocha, H. V. A., Resende, J. A. L. C., Ferreira, G. B., & De Figuereido Teixeira, A. M. R. (2014). An insight into carvedilol solid forms: Effect of supramolecular interactions on the dissolution profiles. *CrystEngComm., 16*, 3168–3179. https://doi.org/10.1039/c3ce42403k

Ramadon, D., Permana, A. D., Courtenay, A. J., McCrudden, M. T. C., Tekko, I. A., McAlister, E., … Donnelly, R. F. (2020). Development, evaluation, and pharmacokinetic assessment of polymeric microarray patches for transdermal delivery of vancomycin hydrochloride. *Molecular Pharmaceutics, 17*, 3353–3368. https://doi.org/10.1021/acs.molpharmaceut.0c00431

Ravindran Maniam, M. M., Loong, Y. H., & Samsudin, H. (2022). Understanding the formation of β-cyclodextrin inclusion complexes and their use in active packaging systems. *Starch - Stärke, 74*, 2100304. https://doi.org/10.1002/STAR.202100304

Ribeiro, L. S. S., Ferreira, D. C., & Veiga, F. J. B. (2003). Physicochemical investigation of the effects of water-soluble polymers on vinpocetine complexation with β-cyclodextrin and its sulfobutyl ether derivative in solution and solid state. *European Journal of Pharmaceutical Sciences., 20*, 253–266. https://doi.org/10.1016/S0928-0987(03)00199-4

Ripolin, A., Quinn, J., Larrañeta, E., Vicente-Perez, E. M., Barry, J., & Donnelly, R. F. (2017). Successful application of large microneedle patches by human volunteers. *International Journal of Pharmaceutics, 521*, 92–101. https://doi.org/10.1016/j.ijpharm.2017.02.011

Ruffolo, R. R., & Feuerstein, G. Z. (1997). Pharmacology of carvedilol: Rationale for use in hypertension, coronary artery disease, and congestive heart failure. *Cardiovascular Drugs and Therapy, 11*, 247–256. https://doi.org/10.1023/A:1007735729121

Sabri, A. H. B., Anjani, Q. K., & Donnelly, R. F. (2021). Synthesis and characterization of sorbitol laced hydrogel-forming microneedles for therapeutic drug monitoring. *International Journal of Pharmaceutics, 607*, Article 121049. https://doi.org/10.1016/j.ijpharm.2021.121049

Sabri, A. H., Cater, Z., Gurnani, P., Ogilvie, J., Segal, J., Scurr, D. J., & Marlow, M. (2020). Intradermal delivery of imiquimod using polymeric microneedles for basal cell carcinoma. *International Journal of Pharmaceutics, 589*, Article 119808. https://doi.org/10.1016/J.IJPHARM.2020.119808

Saokham, P., Burapapadh, K., Praphanwittaya, P., & Loftsson, T. (2020). Characterization and evaluation of ternary complexes of ascorbic acid with γ-cyclodextrin and poly(vinyl alcohol). *International Journal of Molecular Sciences, 21*, 1–14. https://doi.org/10.3390/ijms21124399

Saokham, P., Muankaew, C., Jansook, P., & Loftsson, T. (2018). Solubility of cyclodextrins and drug/cyclodextrin complexes. *Molecules., 23*, 1–15. https://doi.org/10.3390/molecules23051161

Savarese, G., & Lund, L. H. (2017). Global public health burden of heart failure. *Cardiac Failure Review, 3*, 7. https://doi.org/10.15420/CFR.2016:25:2

Schwinger, R. H. G. (2021). Pathophysiology of heart failure. *Cardiovascular Diagnosis and Therapy, 11*, 263–276. https://doi.org/10.21037/CDT-20-302

Shah, N. K., Smith, S. M., Nichols, W. W., Lo, M. C., Ashfaq, U., Satish, P., … Epstein, B. J. (2011). Carvedilol reduces aortic wave reflection and improves left ventricular/vascular coupling: A comparison with atenolol (CENTRAL study). *Journal of Clinical Hypertension, 13*, 917–924. https://doi.org/10.1111/j.1751-7176.2011.00549.x

Sharma, M., Sharma, R., Jain, D. K., & Saraf, A. (2019b). Enhancement of oral bioavailability of poorly water soluble carvedilol by chitosan nanoparticles: Optimization and pharmacokinetic study. *International Journal of Biological Macromolecules, 135*, 246–260. https://doi.org/10.1016/j.ijbiomac.2019.05.162

Sharma, M., Sharma, R., Kumar, D., & Saraf, A. (2019a). Enhancement of oral bioavailability of poorly water soluble carvedilol by chitosan nanoparticles: Optimization and pharmacokinetic study. *International Journal of Biological Macromolecules, 135*, 246–260. https://doi.org/10.1016/j.ijbiomac.2019.05.162

Skotnicki, M., Czerniecka-Kubicka, A., Neilsen, G., Woodfield, B. F., & Pyda, M. (2022). Application of advanced thermal analysis for characterization of crystalline and amorphous phases of carvedilol. *Journal of Pharmaceutical and Biomedical Analysis, 217*, Article 114822. https://doi.org/10.1016/j.jpba.2022.114822

Stella, V. J., Rao, V. M., Zannou, E. A., & Zia, V. (1999). Mechanisms of drug release from cyclodextrin complexes. *Advanced Drug Delivery Reviews, 36*, 3–16. https://doi.org/10.1016/S0169-409X(98)00052-0

Tanwar, Y. S., Chauhan, C. S., & Sharma, A. (2007). Development and evaluation of carvedilol transdermal patches. *Acta Pharmaceutica, 57*, 151–159. https://doi.org/10.2478/v10007-007-0012-x

Tekko, I. A., Vora, L. K., Volpe-zanutto, F., Moffatt, K., Jarrahian, C., Mccarthy, H. O., & Donnelly, R. F. (2022). Novel bilayer microarray patch-assisted long-acting micro-depot cabotegravir intradermal delivery for HIV pre-exposure prophylaxis. *Advanced Functional Materials, 32*, 2106999. https://doi.org/10.1002/adfm.202106999

Todo, H. (2017). Transdermal permeation of drugs in various animal species. *Pharmaceutics., 9*, 1–11. https://doi.org/10.3390/pharmaceutics9030033

Tsuchido, Y., Fujiwara, S., Hashimoto, T., & Hayashita, T. (2017). Development of supramolecular saccharide sensors based on cyclodextrin complexes and self-assembling systems. *Chemical and Pharmaceutical Bulletin (Tokyo), 65*, 318–325. https://doi.org/10.1248/cpb.c16-00963

Ubaidulla, U., Reddy, M. V. S., Ruckmani, K., Ahmad, F. J., & Khar, R. K. (2007). Transdermal therapeutic system of carvedilol: Effect of hydrophilic and hydrophobic matrix on in vitro and in vivo characteristics. *AAPS PharmSciTech, 8*, 2–9. https://doi.org/10.1208/pt0801002

Utomo, E., Domínguez-Robles, J., Moreno-Castellanos, N., Stewart, S. A., Picco, C. J., Anjani, Q. K., … Larrañeta, E. (2022). Development of intranasal implantable devices for schizophrenia treatment. *International Journal of Pharmaceutics, 624*, Article 122061. https://doi.org/10.1016/J.IJPHARM.2022.122061

Vieira, A. C. C., Ferreira Fontes, D. A., Chaves, L. L., Alves, L. D. S., De Freitas Neto, J. L., De La Roca Soares, M. F., … Rolim-Neto, P. J. (2015). Multicomponent systems with cyclodextrins and hydrophilic polymers for the delivery of Efavirenz. *Carbohydrate Polymers, 130*, 133–140. https://doi.org/10.1016/j.carbpol.2015.04.050

Volpe-Zanutto, F., Vora, L. K., Tekko, I. A., McKenna, P. E., Permana, A. D., Sabri, A. H., … Donnelly, R. F. (2022). Hydrogel-forming microarray patches with cyclodextrin drug reservoirs for long-acting delivery of poorly soluble cabotegravir sodium for HIV pre-exposure prophylaxis. *Journal of Controlled Release, 348*, 771–785. https://doi.org/10.1016/J.JCONREL.2022.06.028

Vora, L. K., Moffatt, K., Tekko, I. A., Paredes, A. J., Volpe-Zanutto, F., Mishra, D., … Donnelly, R. F. (2021). Microneedle array systems for long-acting drug delivery. *European Journal of Pharmaceutics and Biopharmaceutics., 159*, 44–76. https://doi.org/10.1016/J.EJPB.2020.12.006

Wenz, G. (2012). Influence of intramolecular hydrogen bonds on the binding potential of methylated β-cyclodextrin derivatives. *Beilstein Journal of Organic Chemistry., 8*, 1890–1895. https://doi.org/10.3762/bjoc.8.218

Wüpper, S., Lüersen, K., & Rimbach, G. (2021). Cyclodextrins, natural compounds, and plant bioactives—A nutritional perspective. *Biomolecules, 11*, 401, 11 (2021) 401 https://doi.org/10.3390/BIOM11030401.

Yao, G., Quan, G., Lin, S., Peng, T., Wang, Q., Ran, H., … Wu, C. (2017). Novel dissolving microneedles for enhanced transdermal delivery of levonorgestrel: In vitro and in vivo characterization. *International Journal of Pharmaceutics, 534*, 378–386. https://doi.org/10.1016/J.IJPHARM.2017.10.035

Yildiz, Z. I., Celebioglu, A., Kilic, M. E., Durgun, E., & Uyar, T. (2018). Fast-dissolving carvacrol/cyclodextrin inclusion complex electrospun fibers with enhanced thermal stability, water solubility, and antioxidant activity. *Journal of Materials Science, 53*, 15837–15849. https://doi.org/10.1007/S10853-018-2750-1/FIGURES/9

Zaid Alkilani, A., Hamed, R., Al-Marabeh, S., Kamal, A., Abu-Huwaij, R., & Hamad, I. (2018). Nanoemulsion-based film formulation for transdermal delivery of carvedilol. *Journal of Drug Delivery Science and Technology, 46*, 122–128. https://doi.org/10.1016/J.JDDST.2018.05.015

Zhang, J., Jiang, P., Sheng, L., Liu, Y., Liu, Y., Li, M., … Liu, W. (2021). A novel mechanism of carvedilol efficacy for Rosacea treatment: Toll-like receptor 2 inhibition in macrophages. *Frontiers in Immunology, 12*, 2777. https://doi.org/10.3389/FIMMU.2021.609615/BIBTEX

Zhang, Y. H., Tian, Y., & Campbell, S. A. (2018). Finite element analysis of hollow HfO2 microneedles for transdermal drug delivery. *Biomedical Microdevices*, 1–6. https://doi.org/10.1109/CISP-BMEI.2017.8302245, 2018-Janua.